CHAPTER IV
PROCESS AND MORPHOLOGY RELATIONSHIP OF POLYSTYRENE GRAFTED WITH BIOCOMPATIBLE POLYMER ELECTROSPUN NANOFIBERS

4.1 ABSTRACT

Electrospinning is a successful process for the production of ultrafine fibers. This process can be used to produce a non-woven membrane composed of electrospun fibers with diameters in the sub-micron range. The resulting material has a high surface area to volume ratio and a high length to diameter ratio which are properties well suited to a variety of applications e.g., filtration membranes, wound dressing scaffolds and drug delivery devices. In this research, the effects of system and processing parameters, including concentration, applied voltage and salt addition on the morphology of the polystyrene grafted with poly(ε-caprolactone) and polystyrene grafted with poly(ε-caprolactam) eletrospun nanofibers were studied. Scanning electron microscopy was used to observe the morphology and fiber diameter of the fibers. From the study, appropriate conditions for electrospinning of PS-g-PCL and PS-g-Nylon were obtained. The average fiber diameter was between 490 nm and 6300 μm. At high concentration and applied voltage the fiber exhibit smooth and less-bead structure but fiber diameter becomes larger. Moreover, after adding a small amount of NaCl, the spinnability of the fiber was improved.

KEYWORDS: electrospinning process, nanofibers, polystyrene, biocompatible polymer

4.2 INTRODUCTION

Many different techniques have been developed to produce nanostructured materials. The electrospinning process has attracted a great deal of attention to produce non-woven membranes of nanofibers. This process can produce polymer

fibers in the nanometer diameter range and can be utilized to assemble fibrous polymer mats composed of fiber diameter lower than 100 nm. The small diameter provides a high surface area to volume ratio, and a high length to diameter ratio. These characteristics are well suitable in variety of applications, such as protective shields in special fabrics, filter media for submicron particles in separation industry, composite reinforcement, especially in biomedical applications including anti-adhesion membranes, wound dressing scaffold, drug delivery, artificial blood vessels and organs.

The electrospinning process has been realized by applying a high voltage to a capillary filled with the polymer fluid. At the end of the capillary, polymer fluid is held by its surface tension. As the intensity of the electric field is increased, the hemispherical surface of fluid at the tip of capillary elongates to form a conical shape (Taylor cone). When the repulsive electrostatic force overcomes the surface tension, charge jet of fluid will be ejected from the tip. The jet breaks up into droplets as a result of surface tension in the case of low viscosity liquids. For high viscosity liquids the jet does not break up, but travels as a jet to the grounded target. The first case is known as electrospraying and is used in many industries to obtain aerosols composed of sub-micron drops with narrow distributions. When applied to polymer solutions and melts, the second case is known as electrospinning and it generates polymer fibers that are sub-micron in diameter. The resulting fibers after solvent evaporatation are collected on the grounded plate, which can be covered with a fabric or may be the rotating cylinder covered with a grounded aluminium sheet.

The parameters and processing variables affecting the electrospinning process are divided into two types. System parameters such as molecular weight of polymer, viscosity of polymer solution, conductivity and surface tension. Process parameters such as electric potential, flow rate and concentration, distance between the capillary and the collector, ambient parameters and finally motion of target screen.

J.M. Deitzel *et al.* (2001) evaluated systematically the effects of two of the most important processing parameters: spinning voltage and solution concentration, on the morphology of the PEO fibers formed. They found that spinning voltage was strongly correlated with an increase in the number of bead defects forming along the electrospun fibers, and that current measurements may be used to signal the onset of

the processing voltage at which the bead defect density increases substantially. Solution concentration has been found to most strongly affect fiber size, with fiber diameter increasing with increasing solution concentration according to a power law relationship. Similar results were also observed by E.R. Kenawy *et al.* (2003). They also indicated that the average fiber diameters of the electrospun poly(ethylene-co-vinyl alcohol) fibers increase with increasing polymer concentration.

Effects of solution properties and processing parameters on the structure and morphology of the electrospun biodegradable membrane like poly(D-lactic acid) and poly(L-lactic acid) were investigated by X. Zong *et al.* (2002). Results obtained demonstrated that the morphology of electrospun polymer fibers depended on the strength of the electric field, the solution viscosity (e.g. concentration), the charge density of the solution (by salt addition), and the solution feeding rate. It was shown that higher concentration and higher charge density of the solution favored the formation of uniform nanofibers without bead-like textures. The diameter of the nanofibers increased with electrospinning voltage as well as feeding rate of the solution. The addition of a small amount of salts or antibiotic drugs was found to greatly change the morphology of electrospun PDLA fibers from beads-on-fiber structure to uniform fiber-structure. The diameters of the nanofibers also decreased with the addition of salts. In addition, different salts exhibited different effects on the morphology of the electrospun fibers. B. Kim *et al.* (2005) explained the effect of salt on morphology of poly(acrylic acid) nanofibers that the characteristic morphology change of PAA nanofibers may be caused by the chain conformation and conductivity changes of PAA solutions with changes of ionic strength.

Zhang *et al.* (2005) studied the effects of instrument parameters including electric voltage, tip–target distance, flow rate and solution parameters such as concentration on the morphology of electrospun poly(vinyl alcohol) fibers. Results showed that, when PVA with higher degree of hydrolysis (DH) of 98% was used, tip–target distance exhibited no significant effect on the fiber morphology, however the morphological structure can be slightly changed by changing the solution flow rate. At high voltages above 10 kV, electrospun PVA fibers exhibited a broad diameter distribution. With increasing solution concentration, the morphology was changed from beaded fiber to uniform fiber and the average fiber diameter could be

increased from 87 ± 14 nm to 246 ± 50 nm. It was also found that additions of sodium chloride and ethanol had significant effects on the fiber diameter and the morphology of electrospun PVA fibers because of the different solution conductivity, surface tension and viscosity. K. H. Lee *et al.* (2003) electrospun poly(ε-caprolactone) from PCL solution in the mixture of methylene chloride and dimethylformamide(DMF). They found that the spinnability and the diameter of the obtained fibers dramatically decreased with increasing DMF content, due to the increased conductivity dielectricity of the resulting solution.

Although it has been shown in the literature in the past years that the various aspects of electrospun fibers have been explored in the different conditions, the morphology of electrospun fibers effected by process parameter for different polymer solvent systems are still worthy of further investigation. In this research polystyrene-graft-poly(ε-caprolactone) and polystyrene-graft-poly(ε-caprolactam) were processed by electrospinning to obtain nanofibers. Variation of processing conditions, and their effects on the structure and morphology of resulting fibers will be studied.

4.3 EXPERIMENTAL

4.3.1 Materials

4.3.1.1 Reagent

Propionyl chloride (98%, Fluka), $AlCl_3$ (97%, Fluka), Nitrobenzene (98%, Merck), Tin(II) 2-ethylhexanoate (stannous octoate, $SnOct_2$, 95%, Aldrich), $LiAlH_4$ (95%, ACROS), Dichloromethane (99.8%, Lab Scan), Tetrahydrofuran (99.8%, Lab Scan), Toluene (99.5%, Lab Scan), Ethanol (99.9%, Aldrich), Dicumyl peroxide (98%, Fluka), Є-caprolactone (99%, Fluka), Polystyrene (PS) and Є-caprolactam were used as received. All syntheses were carried out under purified nitrogen gas.

4.3.1.2 Starting polymers

Polystyrene chains (MW=334,492) were cut by dicumyl peroxide 0.5% (w/w) in dichloromethane at room temperature for 30 minutes and frozen in refrigerator. After chain cutting, Mw of polystyrene was 269,356.

4.3.2 Equipments

4.3.2.1 FTIR/HATR spectroscopy

FTIR spectra were obtained with a Thermo Nicolet spectrometer (NEXUS 670 FT-IR). The spectra were collected in the wave number range 4000-400 cm^{-1} and using KBr pellets.

4.3.2.2 NMR spectroscopy

^1H NMR spectra were measured in $CDCl_3$ in 5-mm glass tubes using a Bruker DPX 300 spectrometer at frequencies 300.13 MHz of frequency and 16 number of scan.

4.3.2.3 Gel Permeation Chromatography (GPC)

All polymers were characterized by GPC (SHIMADZU ClassVP) in THF at room temperature at flow rate of 0.8 ml/min using a set of Water Styragel® HT4 columns. Polystyrene standards for PS/THF system were used to calculate apparent values of molecular weights.

4.3.2.4 Scanning Electron Microscope (SEM)

The morphology of electrospun fibers was observed by using scanning electron microscope (SEM; JSM-6400, JEOL) at voltage of 15 kV. The speciment for SEM were prepared by cutting an aluminum sheet covered with the as-spun fibers and attaching on a SEM stub. Each specimen was gold-coated for 4 minutes.

4.3.2.5 Differential Scanning Calorimetry (DSC)

The melting temperature were determined by differential scanning calorimetry. The melting points were defined as the peak of the endothermal curve. The DSC measurements were carried out with a Perkin-Elmer DSC7 differential scanning calorimeter under N_2 purge, at heating rate 10°C/min. The temperature and heating flow calibration were performed with indium. The scanning range was from 30-250°C

4.3.2.6 Thermal Gravimetry – Dynamic Temperature Analysis (TG-DTA)

Thermal Gravimetry – Dynamic Temperature Analysis technique was used to determine thermal stability and the decomposition temperature of graft copolymers. Perkin-Elmer thermal gravimetry – dynamic temperature

analyzer characterize graft copolymers at heating rate 10°C/min under the nitrogen purge with a purge rate of 200 ml/min. The mass change with increasing temperature was monitored and recorded. The decomposition temperature (Td) was obtained from the derivative TG-DTA thermogram. The samples were in solid state.

4.3.2.7 X-ray Diffractometer (XRD)

XRD spectra were recorded by using a D/MAX-2000 series of Rigaku/X-ray Diffratometer that provides X-ray of Cu K-alpha at 40 kV/30 mA. The experiment was operated at scan speed 5 degree/min with the 0.02-degree 2Θ-stepwise increment.

4.3.3 Methodology

4.3.3.1 Synthesis of ring-acylated polystyrene (polymer A)

A dichloromethane solution (180 ml) of polystyrene which was cut (20 g, MW=269,356, 0.074 mmol) was added under nitrogen to a stirred solution of propionyl chloride (10 ml, 0.576 mol), $AlCl_3$ (12 g) in nitrobenzene (20 ml) (0.09 mol of $AlCl_3$) and dichloromethane (140 ml). The mixture was stirred for 5 hours at room temperature and then precipitated into acidified 80% ethanol (v/v, 1000 ml; 15 ml of HCl). The resulting product was reprecipitated from THF into 80% ethanol and dried at 40 °C under vacuum Yield: 18.12g (white powder). GPC: MW=325,380.

4.3.3.2 Synthesis of polystyrene ring substituted with 1-hydroxypropyl group (polymer B)

A solution of polymer A (20 g, MW=325,380, 0.061 mmol) in dry THF (160 ml) was added to a suspension of $LiAlH_4$ (10 g, 0.26 mol) in dry THF (340 ml) under nitrogen gas. The mixture was refluxed for 5 h and, after that water (5 ml) was gently added to decompose residual $LiAlH_4$. The mixture was then precipitated into acidified water (1350 ml; 150 ml of HCl), filtered, washed with water and dried. The product was reprecipitated from THF into water and finally dried at 40 °C under vacuum. Yield: 10.03g (white powder). IR (KBr, cm^{-1}): 3415 (broad; υ_{OH}) GPC: MW=338,798.

4.3.3.3 Synthesis of polystyrene-graft-poly(ε-caprolactone)

A mixture of polymer B, ring-substituted with 1-hydroxypropyl groups (3 g, MW=338,798, 0.01 mmol), and Є-caprolactone (9 g, 30 g, and 60 g; ratio 1:3, 1:10 and 1:20, respectively) in toluene was heated at 90 °C under nitrogen gas to dissolve all components and a solution of stannous octoate in toluene (3 ml, 0.9 mmol of $SnOct_2$) was then added. The clear solution was then stirred at 90 °C for 24 h, precipitated into cold (-10 °C) hexane and the product was dried at room temperature under vacuum. Yield (PS:Caprolactone): 16.45g (1:3), 30.74g (1:10), and 55.35g (1:20) (white powder). FTIR (KBr, cm^{-1}): 1727($\upsilon_{C=O}$) GPC: MW=689,493 , 642,860, and 622,882, respectively.

4.3.3.4 Synthesis of polystyrene-graft-polycaprolactam

A mixture of polymer B, ring-substituted with 1-hydroxypropyl groups (1 g, 0.003 mmol), and caprolactam (1 g, 2 g, and 3 g; ratio 1:1, 1:2 and 1:3, respectively) in toluene (10, 20 and 30 ml, respectively) was heated at 90 °C under nitrogen gas to dissolve all components and a solution of stannous octoate in toluene (1 ml, 0.3 mmol of $SnOct_2$) was then added. The clear solution was then stirred at 90 °C for 24 h, precipitated into cold (-10 °C) hexane and the product was dried at room temperature under vacuum. Yield (PS: caprolactam): 1.34g (1:1), 1.83g (1:2), 2.84g (1:3) (pale yellow powder). FTIR (KBr, cm^{-1}): 1653 ($\upsilon_{C=O(amidel)}$). GPC: MW=264,824, 228,859, and 149,131, respectively.

4.3.3.5 Electrospinning process

Polymer solution was prepared for electrospinning at different concentrations. Chloroform and toluene were used as the solvent for PS-g-PCL and PS-g-Nylon respectively. Polymer solution was placed in a 5ml syringe fitted with a needle. Nanofibers were fabricated by electrospinning process at different applied voltage using a positive high voltage power supply (Gamma High Voltage Research). The collection plate of aluminum foil was located at a fixed distance 20 cm from the needle tip. The tilt angle of syringe was 45° from the horizontal baseline. The polymer solution formed Taylor cone at the tip of the needle by combination of gravitational force and electrostatic force. The charged jet ejected to form nanofibers and grounded on the aluminum foil target. As-spun nanofibers were dried under vacuum at room temperature over night.

4.4 RESULTS AND DISCUSSION

4.4.1 Characterization of polystyrene grafted with biocompatible polymer

4.4.1.1 Fourier Transform Infrared Spectroscopy Results

The synthesis of polystyrene grafted with biocompatible polymer started with Friedel-Crafts acylation of polystyrene led to the polymer ring-substituted with propionyl groups. In the second step, carbonyl groups in ring-acylated polystyrene were reduced to hydroxyl groups. The resulting products from both steps were characterized by FTIR spectroscopy. The FTIR spectrum of ring-propionylated polystyrene exhibits an absorption peak at 1684 cm^{-1} attributed to carbonyl stretching, aliphatic hydrocarbon at 2850-2950cm^{-1}, para substituted aromatic hydrocarbon at 3000-3080cm^{-1} and 1800-2000cm^{-1} and mono substituted aromatic hydrocarbon at 700-1600cm^{-1} (Figure 4.1(a)) whereas the FTIR spectrum of 1-hydroxypropyl polystyrene shows complete disappearance of the carbonyl peak in favor of the broad band centered at 3415 cm^{-1}, characteristic of hydroxyl groups (Figure 4.1(b)). The successful product of grafting polystyrene with poly(ε-caprolactone) gave the significant strong peak of carbonyl group at 1727 cm^{-1} and departure of broad hydroxyl band (Figures 4.2-4.4). Polystyrene-graft-poly(ε-caprolactam) have spectrum which demonstrate the carbonyl peak of amide group at 1653 cm^{-1} (Figure 4.5-4.7).

4.4.1.2 NMR Results

In the ^{1}H NMR spectrum (Figure 4.8), the signals characteristic of propionyl protons and aromatic protons ortho to the propionyl group vanished; a new signal appeared at 4.5 ppm, assigned to the OCH proton in the 1-hydroxypropyl group (Figure 4.9). All free hydroxy groups of the hydroxylated PS effectively initiated the ROP of ε-caprolactone or caprolactam. Due to the grafted caprolactone units, the 1-hydroxypropyl group transformed to the Ø-CH(CH_2CH_3)-O- groupings and the signal of the methine proton shifted to 5.60 ppm (Figure 4.10). The signals characteristic of methylene protons in grafted caprolactone units appeared at 4.1, 2.4 and 3.60 ppm; the last value corresponds to the methylene protons in terminal CH_2OH group (Figure 4.10). The signals characteristic of amide

protons in grafted caprolactam units appeared at 2.45, 8.00 and 2.23 ppm; the last value corresponds to the amine protons in terminal -NH_2 group (Figure 4.11).

4.4.1.3 Molecular Weight Measurement

The molecular weight of polymer has a significant influence on the rheological properties, electrical conductivity and the surface tension in the solution. The preceding properties are some of the major parameters governing the electrospinning process. GPC analysis used to characterize the molecular weight of the synthesized-products from each step (Table 4.1). It was shown that the molecular weight of commercial polystyrene is 334,492. After chain cutting molecular weight of polystyrene decreased to 269,356, ring-acylated polystyrene and 1-hydroxy polystyrene were 325,380 and 338,798 respectively. The molecular weight extremely increased in grafting step of PS-g-PCL whereas decreased in case of PS-g-Nylon which may be caused by less proper reaction condition and thermal degradation of polymer chain during grafting reaction.

Furthermore, increasing amount of ε-caprolactone and ε-caprolactam monomer influenced to decrease molecular weight. The decreasing of molecular weight when increased amount of ε-caprolactone and ε-caprolactam monomer may be caused by increasing number of grafting sites that create PCL or Nylon shorter chains on PS main chain instead of continuous growing a long grafting-chain, so the molecular weight measured by GPC of PS-g-PCL and PS-g-Nylon at the higher ratio of monomer are lower than that at the lower ratio of monomer. After electrospinning process the graft copolymers with different molecular weight will probably give different fiber structure.

4.4.2 Characterization of nanofibers

4.4.2.1 Effect of processing parameters

Concentration effect

The SEM micrographs in Figure 4.12-4.21 illustrate the effect of polymer concentration on morphological appearance of the obtained as-spun materials. In the case of PS-g-PCL (Figure 4.12-4.14), all ratios show the same results that fiber diameter could be significantly increased with the increasing

polymer concentration at constant applied voltage of 15kV. Meanwhile, the shape of the beads also changed from spherical to spindle like. Furthermore, in case of PS-g-Nylon, i.e. it appears that a large number of droplets were present at low concentration whereas the combination of smooth and beaded fibers were observed at high concentration (Figures 4.15-4.17). It could be explained that at low concentration or low viscosity, the visoelastic force was not large enough to counter the higher Coulombic force, resulting in the break up of the charged jet into the small droplets. While at higher concentration, the solution has high viscoelastic force to prevent the break up of the charged jet and to allow the Coulombic force to further elongate the charged jet to the ground target. The explanations for increasing of fibers diameter were that as the concentration increased the amount of solvent of charged jet decreased, resulting in the much easier drying of charged jet. However the increased concentration enabled the charged jet to withstand larger stretching force from the Coulombic repulsion thus the larger diameter of the charged jet was observed.

Electrospinning voltage effect

For the effect of applied voltage, SEM micrographs in Figure 4.18 show electrospun fibers of PS-g-PCL 1:20, 25%w/v when the applied voltage increased from 10-25 kV. It appears that fiber formation was improved. The electrospun fiber changes from the bead-like to the smooth fiber and fiber diameter become larger. However, incase of PS-g-Nylon, the electrospun fiber also change from large beads with thin fibers to small beads with larger fibers as voltage increases (Figure 4.19). It could be a result of the increase in the mass throughput in response to the increase in the electrostatic force.

Effect of ionic salt addition

The morphological appearance of the electrospun fibers were changed after add 0.01M NaCl into the polymer solutions (Figures 4.20-4.21). It was shown that the electrospun fibers of PS-g-PCL 1:10, 30%w/v at 15kV (Figure 4.20(b)) changed from bead-like structure to no bead structure after adding 0.01M NaCl. Moreover, in case of electrospun PS-g-Nylon 1:1 (Figure 4.21), fibers were smoother and bead size becomes smaller from 10 μm (without NaCl) to 2.9 μm (with 0.01M NaCl). This behavior can be explained as following. The addition of salt

results in a higher charge density on the surface of charged jet during electrospinning. As the charge carried by the jet increase, higher elongation forces are imposed to the jet under the electrical field. It is known that overall tension in the fibers depend on the self-repulsion of the excess charges on the jet. Thus, as the charge density increases, the beads become smaller and the fiber become smoother. Moreover fiber density seems to be increased by adding salt into polymer solution. The fiber density can be examined by measuring the length between junction of fibers. It was shown that the length between junction tend to decrease after add salt into polymer solution it means that amount of fibers in a unit area is increase (fiber density increase). For PS-g-PCL without adding salt, the length between junction of fibers are 9.554, 17.143 and 15.776 (ratio 1:3, 1:10 and 1:20, respectively) while the systems with 0.01M NaCl, the length between junction are 15.597, 10.309 and 12.126 (ratio 1:3, 1:10 and 1:20, respectively). For PS-g-Nylon (ratio 1:1, 20%), the length between junction of fiber obviously decrease from 17.549 to 9.279 (for system with and without salt, repectively).

4.4.2.2 Differential Scanning Calorimetry (DSC) Results

Figures 4.22-4.24 show DSC profiles of as-synthesized and electrospun fiber of PS-g-PCL. The as-synthesized PS-g-PCL show the endothermic peaks at ~59°C which recognizes as melting temperature of PCL-unit while PS is amorphous polymer so there are no melting peak of PS-unit appears in the profiles. PS composition does not significantly alter the melting of PCL as the profiles demonstrate the melting temperatures of PCL unit at ~59°C equal to Tm of pure poly(ε-caprolactone). The nanofibers were electrospun from 30% PS-g-PCL solution at applied voltage of 15 kV. Electrospun PS-g-PCL ratio 1:3 shows the same melting point as the synthesized material. However melting point of PS-g-PCL ratio 1:10 and 1:20 are lower than that of as-synthesized PS-g-PCL. It means that crystalline structure of electrospun fibers is not well developed. As the electrospinning process let polymer forms fibers which small size lead to the restricted mobility of the polymer chains which did not allowed the growth of well developed lamellar crystals so melting peak shifted to lower temperature. In case of PS-g-Nylon, DSC profile did not validate the thermal property of this material.

4.4.2.3 X-ray Diffraction (XRD) Results

It's corresponding to the results from DSC profiles, XRD patterns of PS-g-PCL (Figure 4.25-4.27) both as-synthesized materials and as-spun fibers show that the peak position are identical so there is no change in crystal structure induced by the electrospinning process. And the diffraction peaks of as-synthesized samples are sharper than peak of as-spun fibers, indicating that the crystalline order in fiber was less than in as-synthesized sample.

4.4.2.4 Thermal Gravimetric Analysis (TGA) Results

The TG-DTA curves of copolymer show the decomposition processes in different temperature ranges of each composition under nitrogen gas. The combustion profile is not only used to explain degradation temperature but also used to confirm the species in the synthesized compound. The TG-DTA curves of all ratio of PS-g-PCL samples (Figures 4.28-4.30) show a two-step decomposition process, first decomposition process occurs at 356.8°C, 332.5°C and 347.5°C for ratio of PS:PCL at 1:3, 1:10 and 1:20 respectively which are degradation temperature of poly(ε-caprolactone). These temperatures are close to Td of pure PCL that is about 402°C. Second decomposition process appears at 427.7°C, 431.4°C and 432.1°C define as the degradation temperatures of PS which actually has Td about 409°C. The weight loss of two-decomposition process obviously corresponds to the ratio of PS and PCL those are 1:3, 1:10 and 1:20. The thermograms of electrospun PS-g-PCL (Figures 4.31-4.33) show the same results as those results of as-synthesized polymers.

In case of PS-g-Nylon, the TG-DTA curves of as-synthesized copolymer of ratio 1:1 and 1:2 showed three decomposition processes (Figure 4.34-4.35). The most change decomposition at 420°C with %weight loss 54.04% and 39.39% (PS:ε-caprolactam1:1 and 1:2 respectively) are the degradation temperature of polystyrene. The decomposition process occurs in temperature range about 100-270°C with %weight loss 16.93% and 28.63% (PS:ε-caprolactam1:1 and 1:2 respectively) can be defined as degradation temperature of monomer or dimer of ε-caprolactam. Moreover there is a small degradation process about 330°C with %weight loss 6.51% and 9.29% (PS:ε-caprolactam1:1 and 1:2 respectively) which

may possibly be poly(ε-caprolactam) with low molecular weight. In case of as-synthesized PS-g-Nylon ratio 1:3 (Figure 4.36), there are two decomposition processes, the first one occurs about 214.1°C with %weight loss 69.78% which demonstrate the degradation temperature of ε-caprolactam oligomer. The second degradation appears at 419.5°C with % weight loss13.98% which certainly be the degradation temperature of polystyrene. Amazingly the thermograms of as-spun PS-g-Nylon are different from the as-synthesized one. In case of electrospun PS-g-Nylon 1:1and 1:2 (Figure 4.37-4.38), the thermograms show 1st transition at about 138-141°C correspond to degradation process of ε-caprolactam monomers. The new degradation process at 467.2°C and 495.0°C (1:1 and 1:2 respectively) that did not appear in the curves of as-synthesized material were defined as degradation temperature of Nylon which generally has Td about 470°C. Moreover the degradation temperature of polystyrene was shifted to the lower temperature. It means that the condition during electrospinning process (e.g. temperature, high voltage) may affect the modification of the species, i.e. the induction of polymerization of ε-caprolactam to Nylon6.

4.5 CONCLUSIONS

The PS-g-PCL and PS-g-Nylon electrospun fibers were successfully fabricated through the electrospinning process by using chloroform and toluene as the solvent. After electrospinning, morphology and properties change of electrospun fibers were thoroughly examined. The effect of polymer concentration, applied voltage and salt addition on the electrospinning process and morphology of fibers were investigated by using SEM. Increasing of the polymer concentration significantly expands the diameter and eliminate bead structure in nanofibers. The electrospinning voltage influenced the increasing of fiber diameter and also improved fiber formation. Moreover, addition small amount of NaCl in the solution can improved the spinninability of electrospun fibers.

DSC and XRD show the results that electrospinning process did not introduce any new crystal structure of materials. According to DSC results, Tm of

PS-g-PCL electrospun fibers were lower than Tm of as-synthesized materials revealing incomplete developed crystalline. The diffraction peak from XRD of PS-g-PCL electrospun fibers were not sharp like that of as-synthesized materials.

TG-DTA results demonstrate that the decomposition process of PS-g-Nylon were changed after electrospinning, there is Td of Nylon appear in case of electrospun fibers whereas it was absent from the thermogram of as-synthesized materials. It means that the condition during electrospinning process (e.g. temperature, high voltage) may affect the modification of the species by enhancing polymerization of ε-caprolactam to nylon.

4.6 ACKNOWLEDGEMENTS

This thesis work is partially funded by Postgraduate Education and Research Programs in Petroleum and Petrochemical Technology (PPT Consortium) and Polymer Processing and Polymer Nanomaterials Rerearch Unit.

Special thanks go to Dr. Ratthapol Rangkupan of the Metallurgy and Material Science Research Institute (MMRI), Chularlongkorn University Petroleum for useful suggestions.

Finally, the author would like to take this opportunity to thank PPC friends, the author had the most enjoyable time working with all of them. Also, the author is greatly indebted to her family for their support, love and understanding.

4.7 REFERENCES

[1] Frenot, A., Chronakis, I.S. (2003) *Current Opinion in Colloid and Interface Science*, 8, 64-75.

[2] Zeng, J., Xu, X., Chen, X., Liang, Q., Bian, X., Yang, L., Jing, X. (2003) *Journal of Controlled Release*, 92, 227-231.

[3] Zeng, J., Xu, X., Chen, X., Liang, Q., Bian, X., Yang, L., Jing, X. (2003) *Journal of Applied Polymer Science*, 89, 1085-1092.

[4] Doshi, J., Reneker, D.H. (1995) *Journal of Electrostatics*, 35, 151-160.

[5] Deitzel, J.M., Kleinmeyer, J., Harris, D., Tan, N.C. (2001) *Polymer*, 42, 261-272.

[6] Kenawy, E.R., Layman, J., Watkins, J., Bowlin, G., Matthews, J., Simpson, D., Wnek, G. (2003) *Biomaterials*, 24, 907-913.

[7] Zong, X., Kim, K., Fang, D., Ran, S., Hsiao, B.S., Chu, B. (2002) *Polymer*, 43, 4403-4412.

[8] Kim, B., Park, H., Lee, S.-H., Sigmund, W.M. (2005) *Materials Letters*, 59, 829-832.

[9] Zhang, C., Yuan, X., Wu, L., Han, Y., Sheng, J. (2005) *European Polymer Journal*, 41, 423-432.

[10] Koski, A., Yim, K., Shivkumar, S. (2004) *Materials Letters*, 58, 493-497.

[11] Lee, K.H., Kim, H.Y., Khil, M.S., Ra, Y.M., Lee, D.R. (2003) Polymer, 44, 1287-1294.

[12] Mit-uppatham, C., Nithitanakul, M., and Supaphol, P., (2004) *Macromolecular Symposia*, 216, 293-299.

Figure 4.1 FTIR spectrum of ring-acylated polystyrene(a) and 1-hydroxy polystyrene(b).

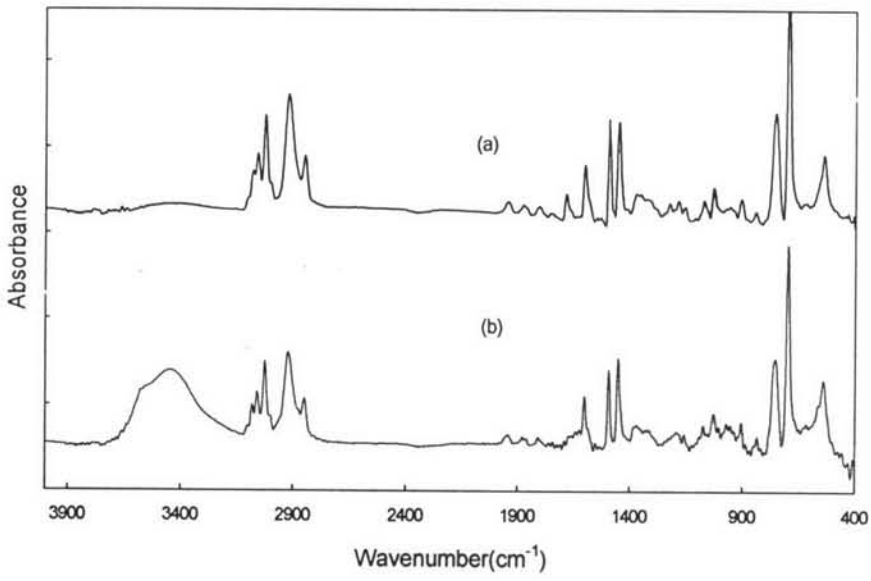

Figure 4.2 FTIR spectrum of PS-g-PCL 1:3.

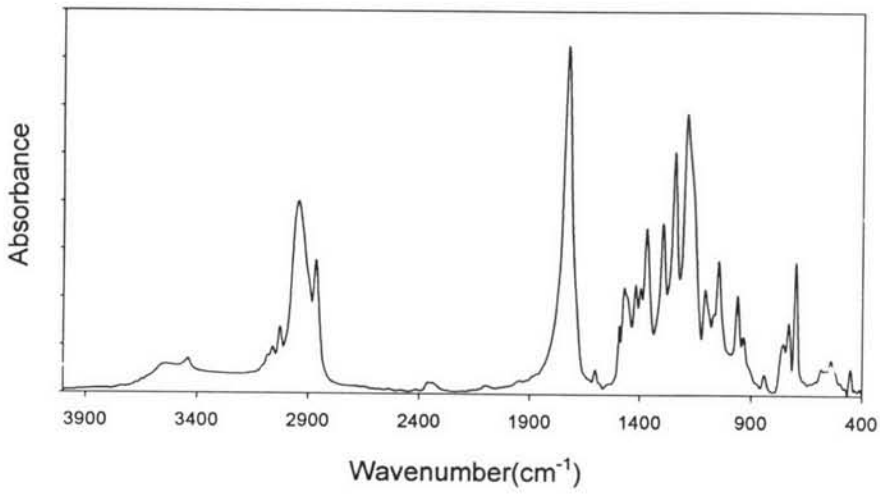

Figure 4.3 FTIR spectrum of PS-g-PCL 1:10.

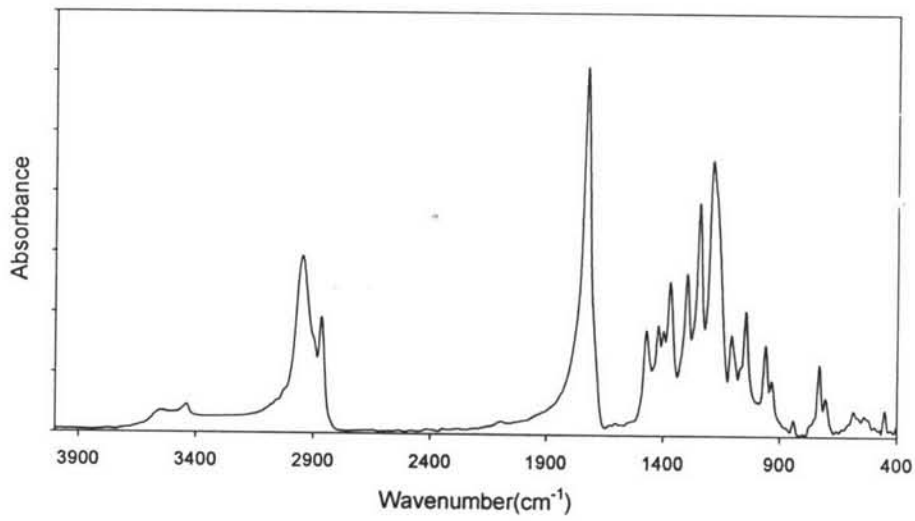

Figure 4.4 FTIR spectrum of PS-g-PCL 1:20.

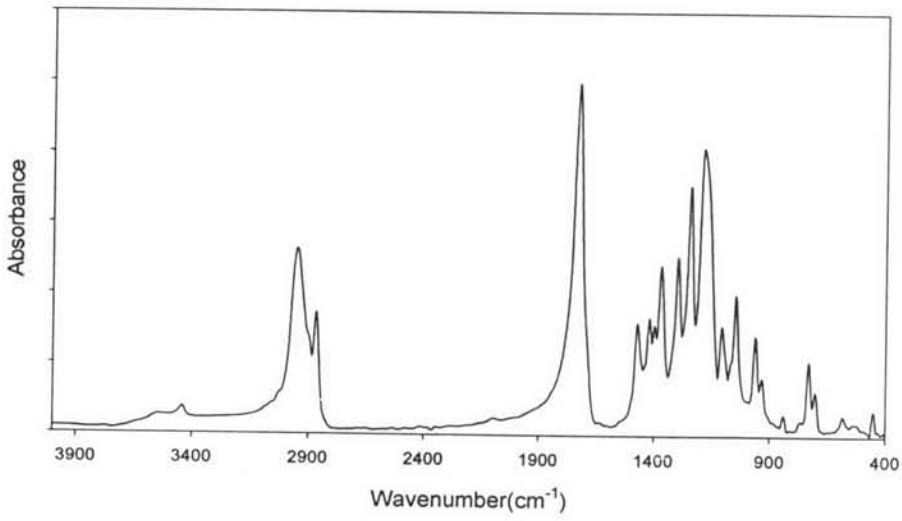

Figure 4.5 FTIR spectrum of PS-g-Nylon 1:1.

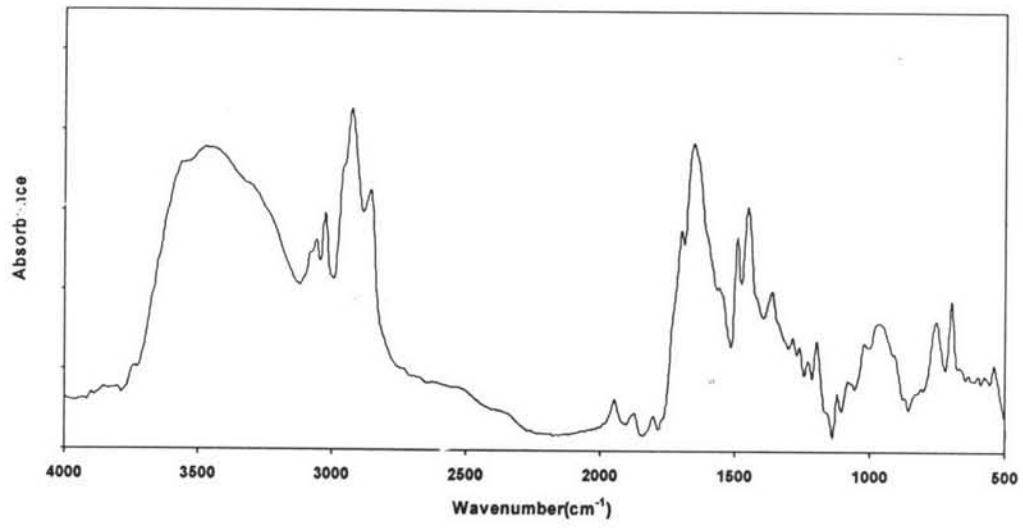

Figure 4.6 FTIR spectrum of PS-g-Nylon 1:2.

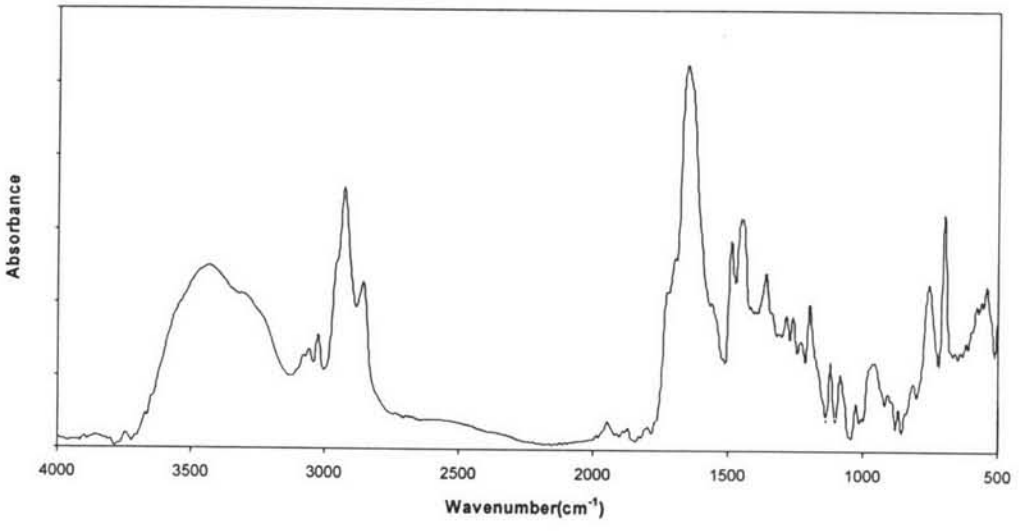

Figure 4.7 FTIR spectrum of PS-g-Nylon 1:3.

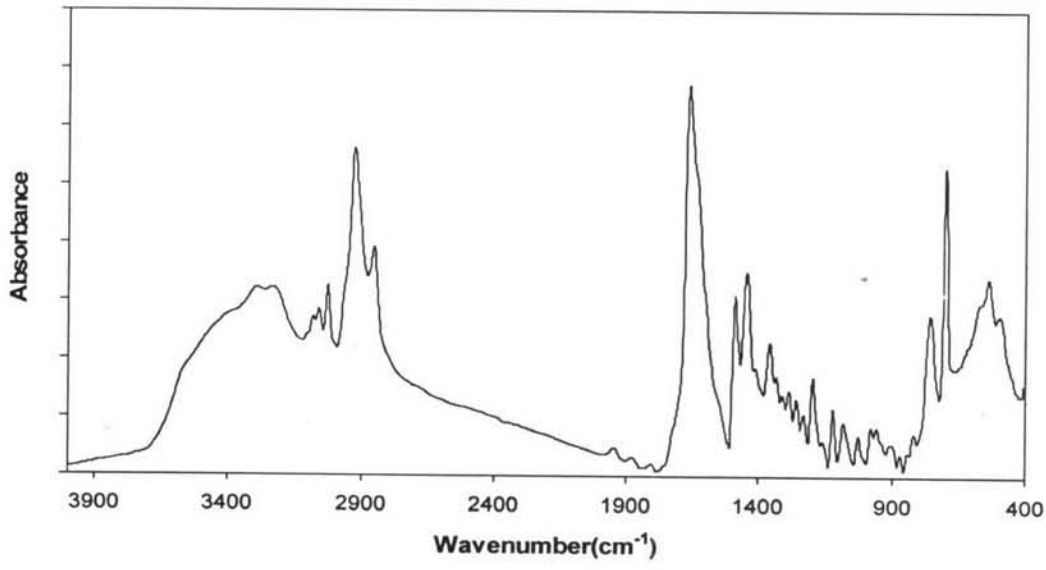

Figure 4.8 ^{1}H NMR spectrum of ring-propionylated polystyrene.

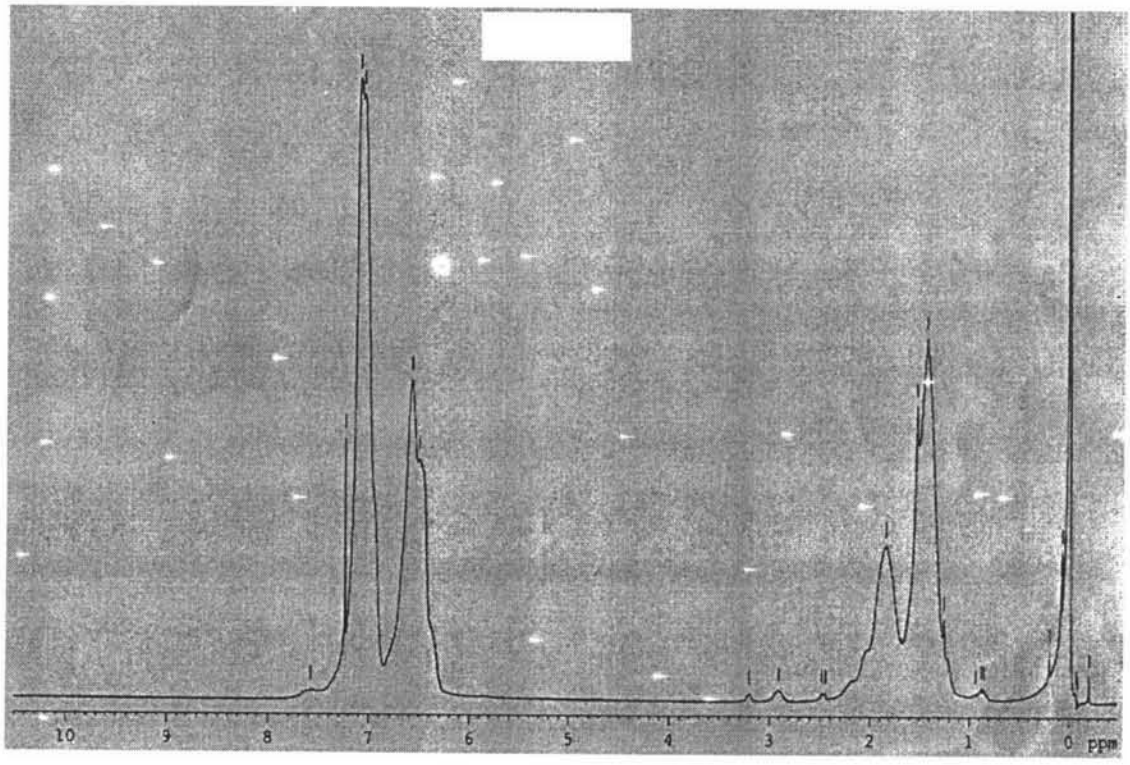

Figure 4.9 ^{1}H NMR spectrum of 1-hydroxy polystyrene.

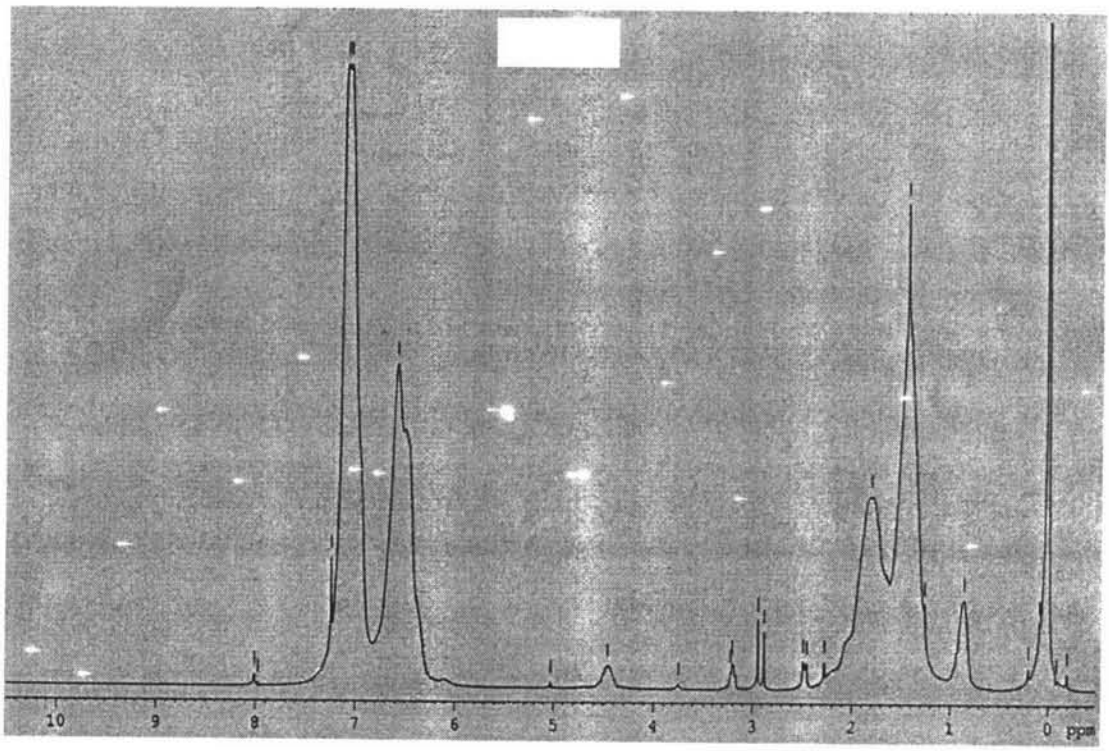

Figure 4.10 ^{1}H NMR spectrum of PS-g-PCL.

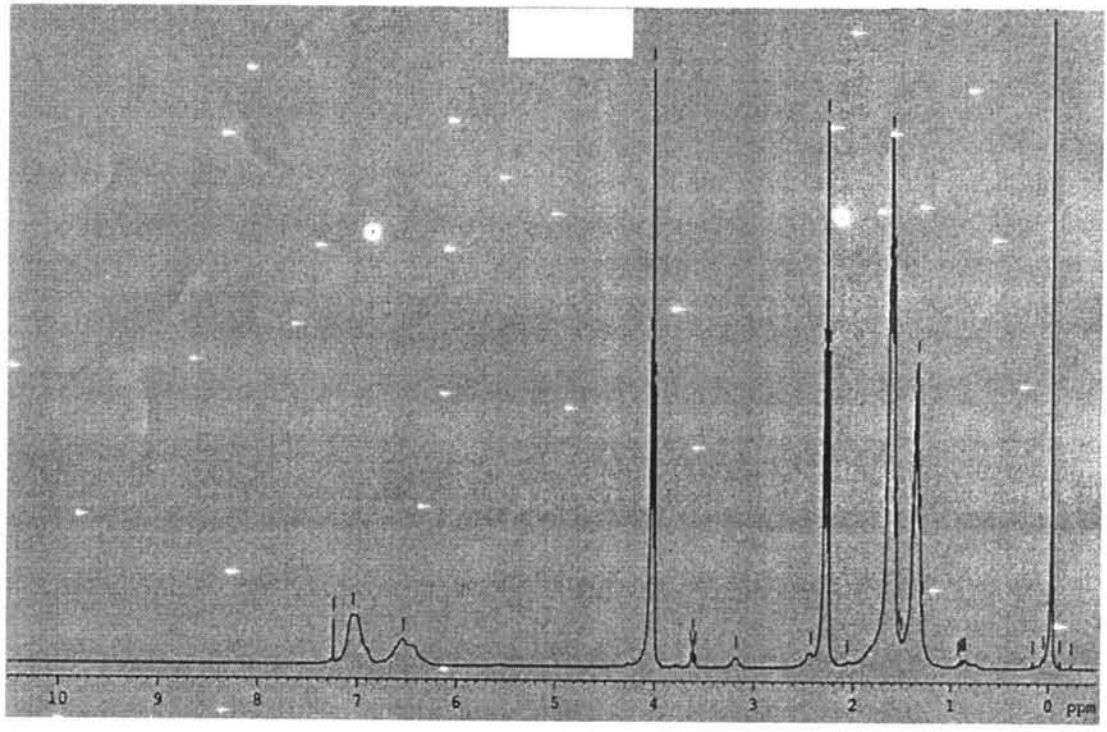

Figure 4.11 ^{1}H NMR spectrum of PS-g-Nylon.

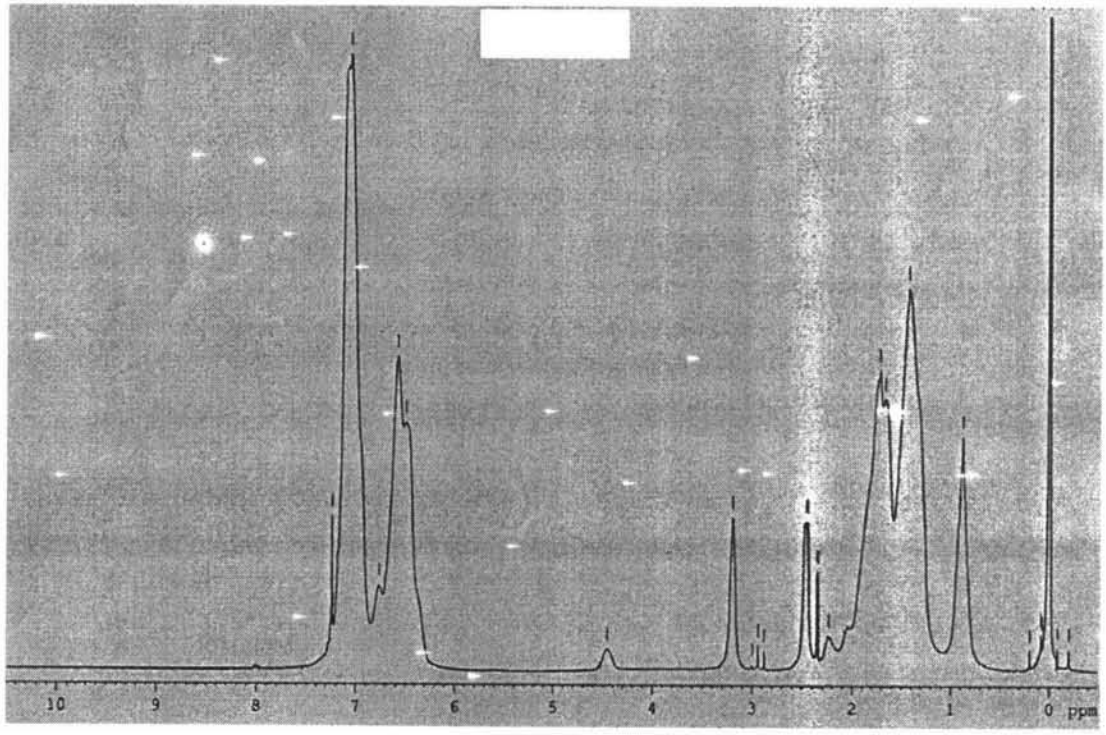

Table 4.1 The retention time and the molecular weight of polymer in THF at room temperature with Gel Permeation Chromatography (rate 0.8 ml/min).

Sample	Retention time	Mw
PS	8.819	334492
PS-cut	8.935	269356
step1	9.071	325380
step2	9.03	338798
PS-g-PCL1:3	7.834	689493
PS-g-PCL1:10	8.068	642860
PS-g-PCL1:20	7.676	622882
PS-g-Nylon1:1	9.876	264824
PS-g-Nylon1:2	9.908	228859
PS-g-Nylon1:3	9.613	149131

Figure 4.12 SEM micrographs of PS-g-PCL (1:3) fiber electrospun at 15kV from polymer concentration: (a) 15wt%; (b) 20wt% and (c) 25wt%.

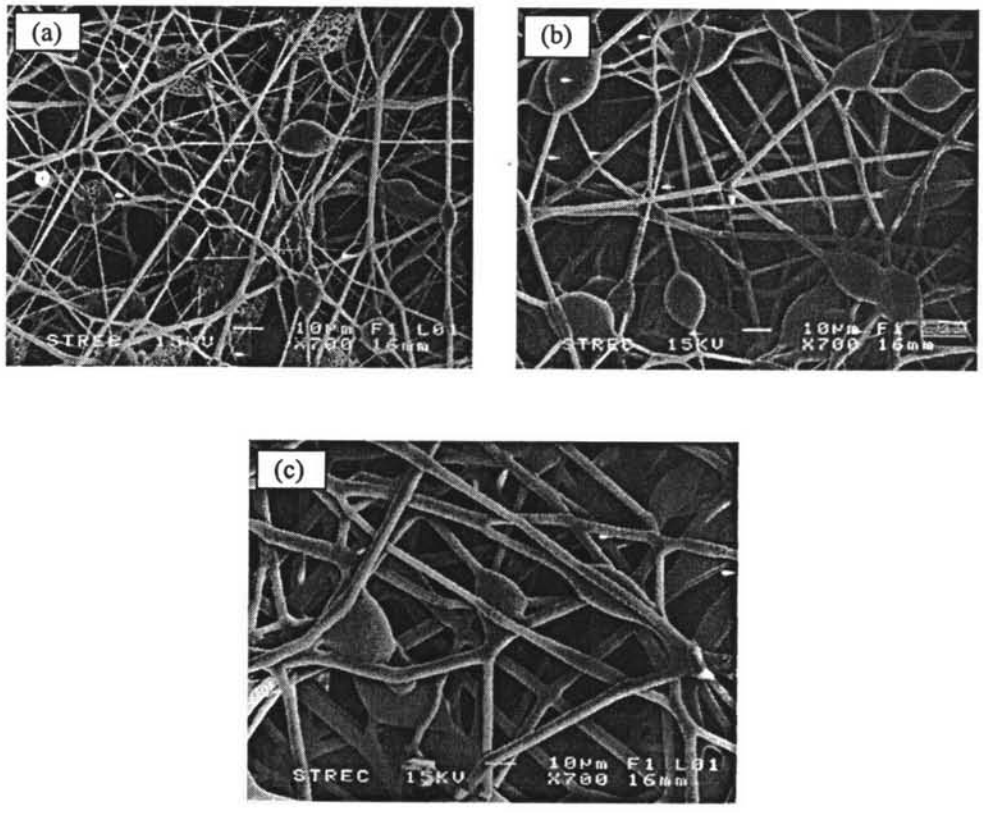

Figure 4.13 SEM micrographs of PS-g-PCL (1:10) fiber electrospun at 15kV from polymer concentration: (a) 20wt%; (b) 25wt% and (c) 30wt%.

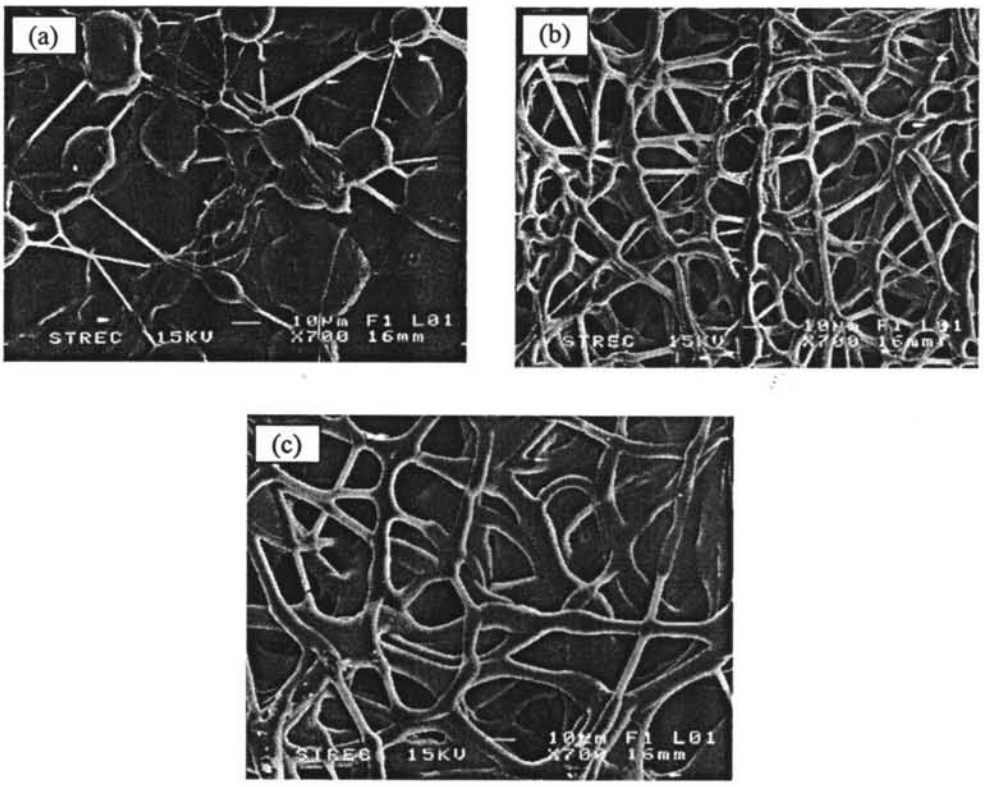

Figure 4.14 SEM micrographs of PS-g-PCL (1:20) fiber electrospun at 15kV from polymer concentration: (a) 20wt%; (b) 25wt% and (c) 30wt%.

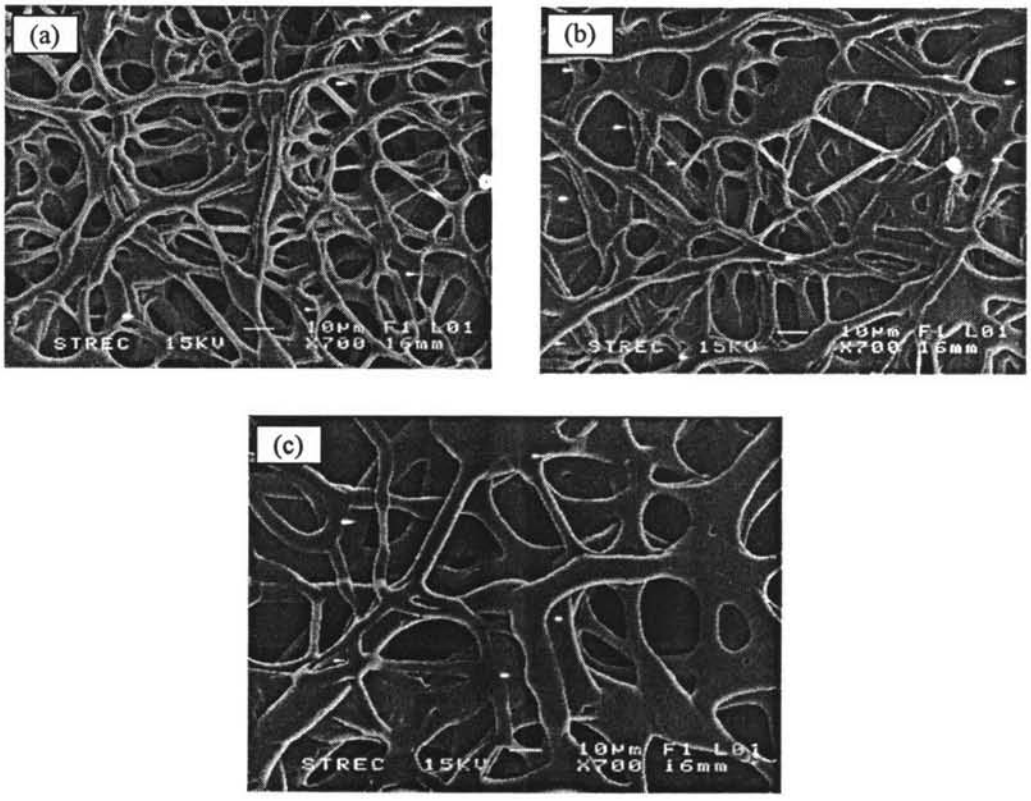

Figure 4.15 SEM micrographs of PS-g-Nylon (1:1) fiber electrospun at 15kV from polymer concentration: (a) 20wt%; (b) 25wt% and (c) 30wt%.

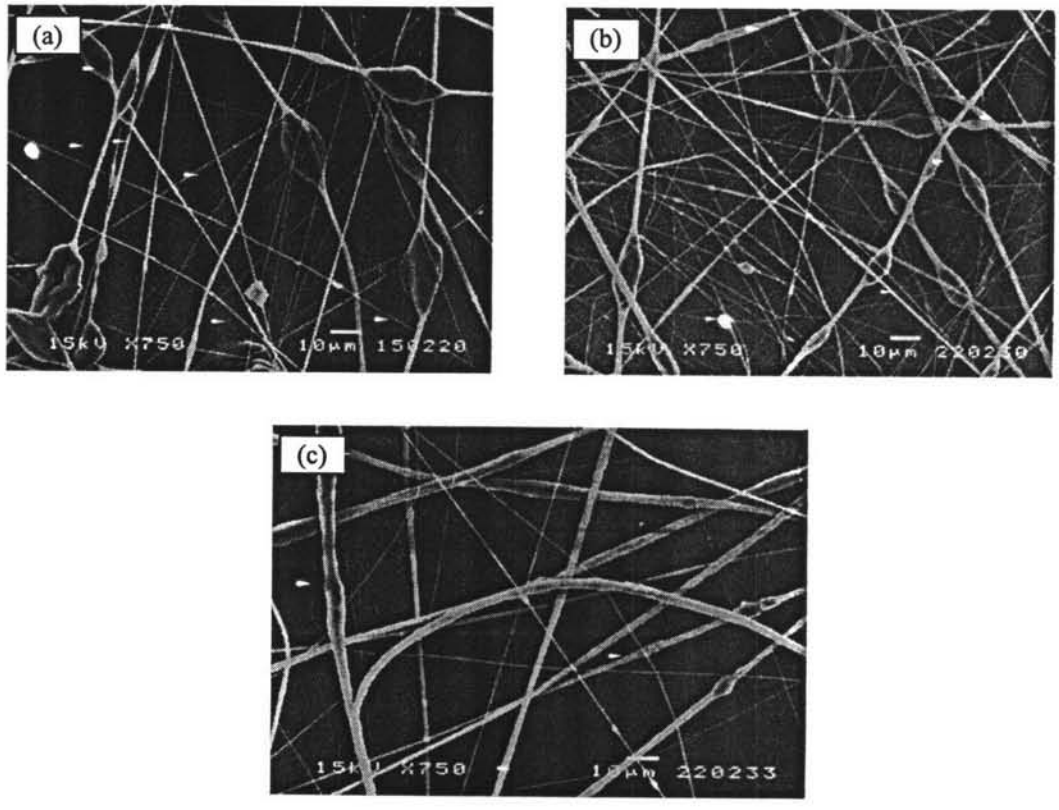

Figure 4.16 SEM micrographs of PS-g-Nylon (1:2) fiber electrospun at 15kV from polymer concentration: (a) 20wt%; (b) 25wt% and (c) 30wt%.

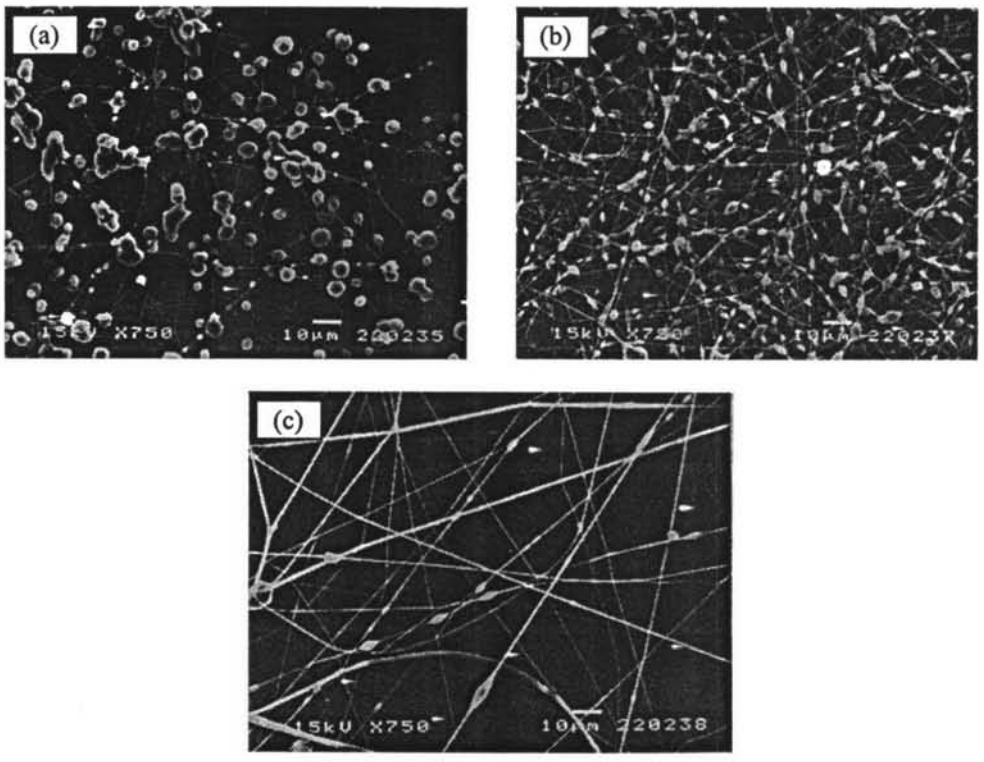

Figure 4.17 SEM micrographs of PS-g-Nylon (1:3) fiber electrospun at 20kV from polymer concentration: (a) 35wt%; (b) 40wt% and (c) 45wt%.

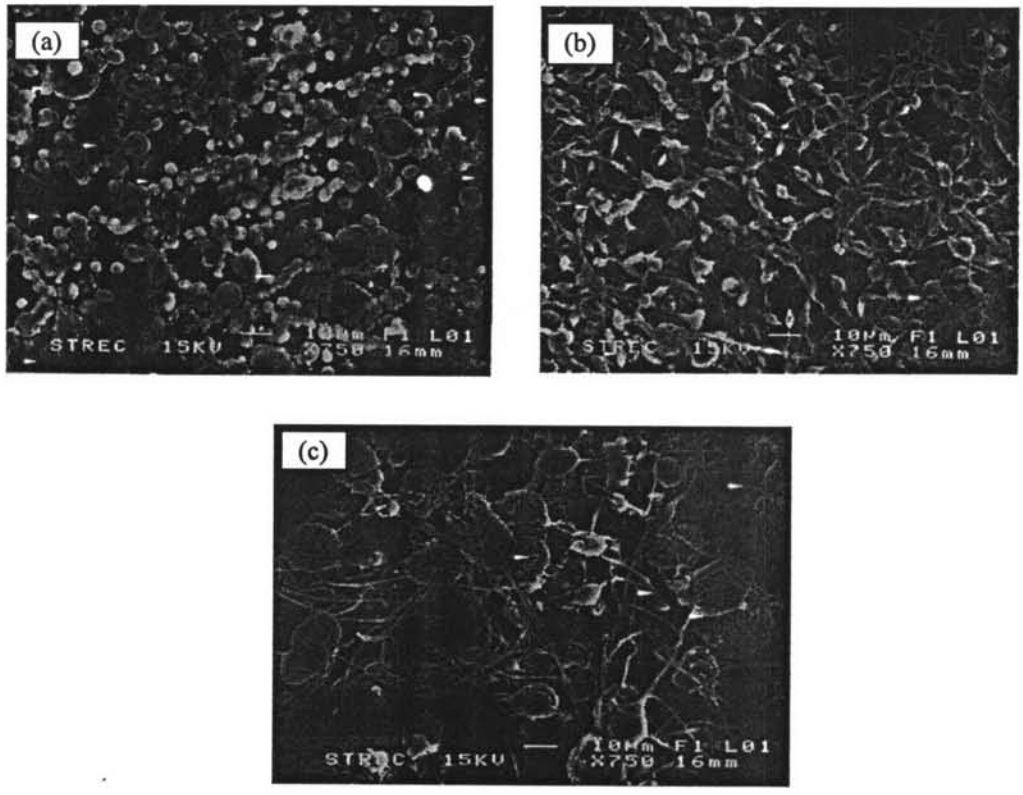

Figure 4.18 SEM micrographs of PS-g-PCL (1:20) fiber electrospun from polymer concentration 25wt% at: (a) 10kV, (b) 15kV, (c) 20kV and (d) 25kV.

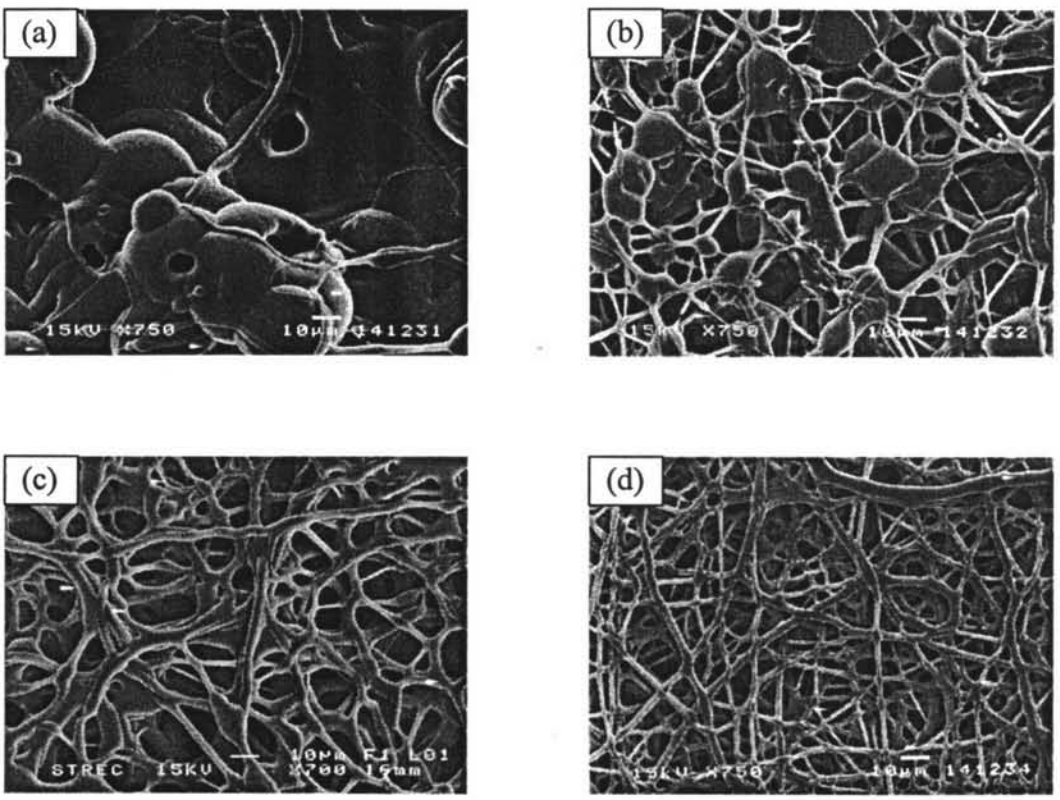

Figure 4.19 SEM micrographs of PS-g-Nylon (1:2) fiber electrospun from polymer concentration 25wt% at: (a) 10kV, (b) 15kV and (c) 20kV.

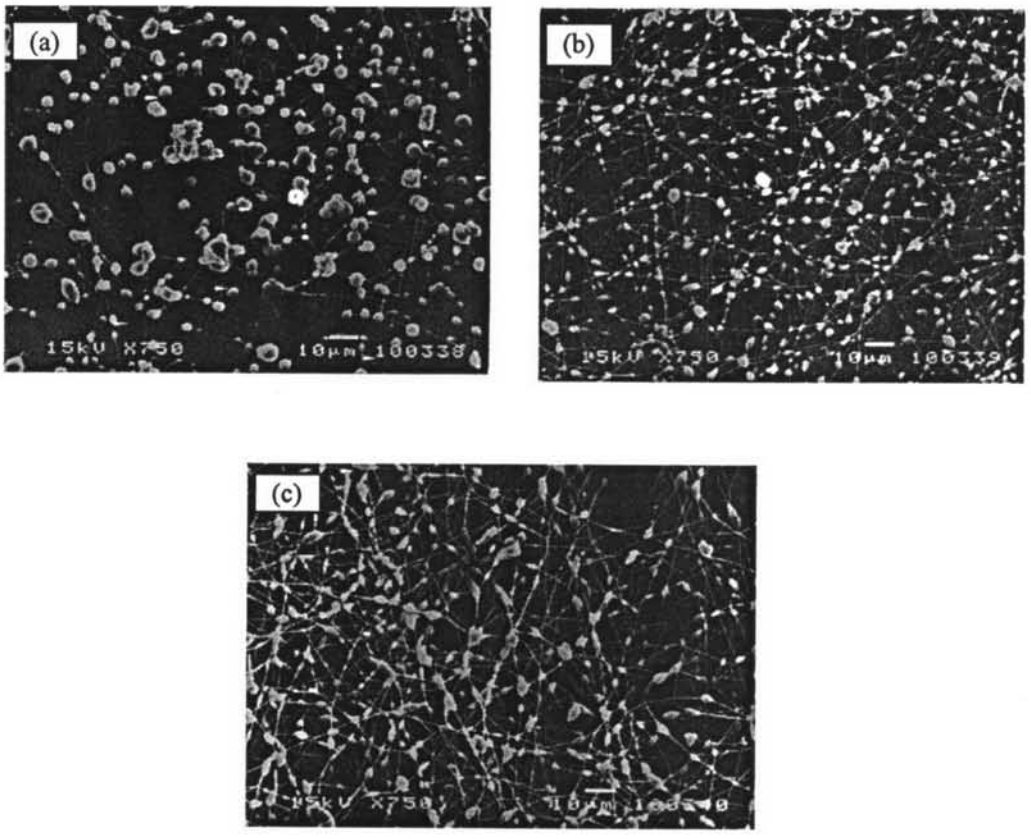

Figure 4.20 SEM micrographs of PS-g-PCL fiber electrospun at 15kV from polymer concentration 30wt% ratio of PS:PCL (a) 1:3, (b) 1:10 and (c) 1:20 comparing between with and without 0.01M NaCl.

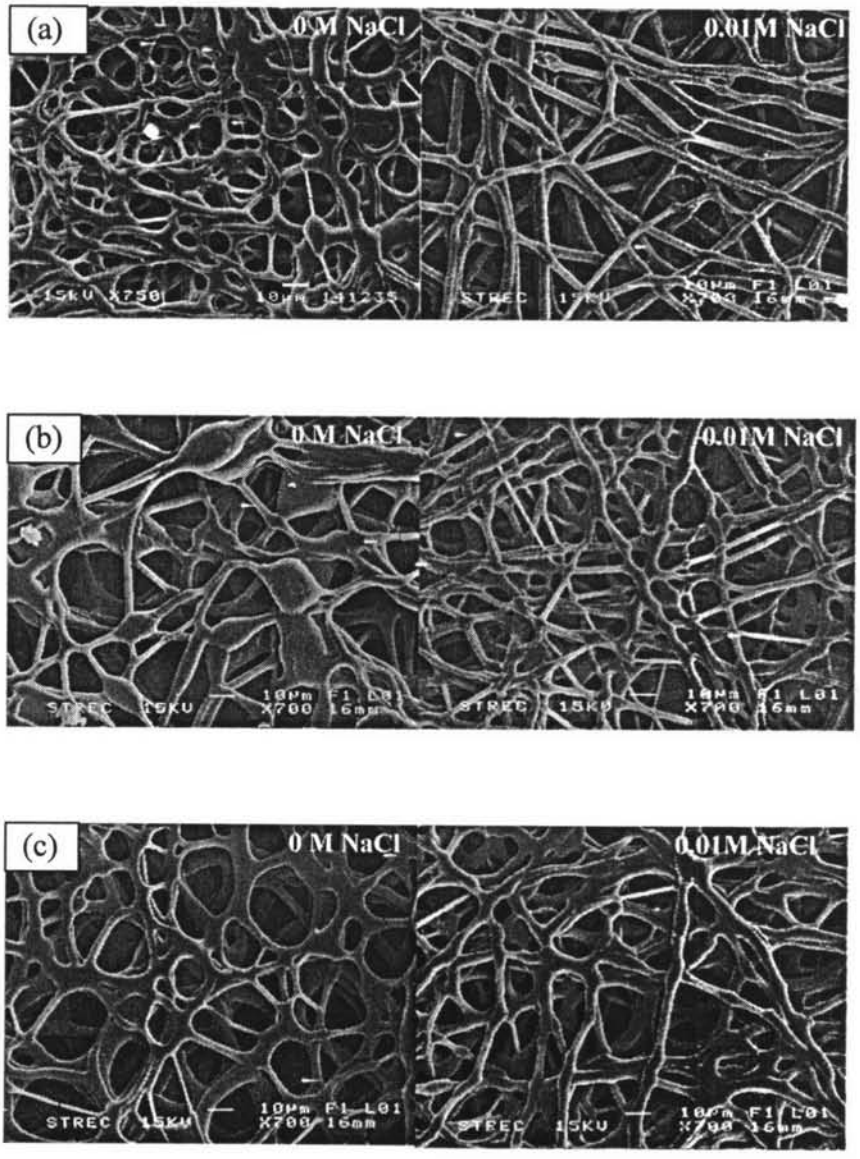

Figure 4.21 SEM micrographs of PS-g-Nylon fiber electrospun at 15kV from polymer concentration 20wt% ratio of PS: ε-caprolactam 1:1 comparing between with and without 0.01M NaCl.

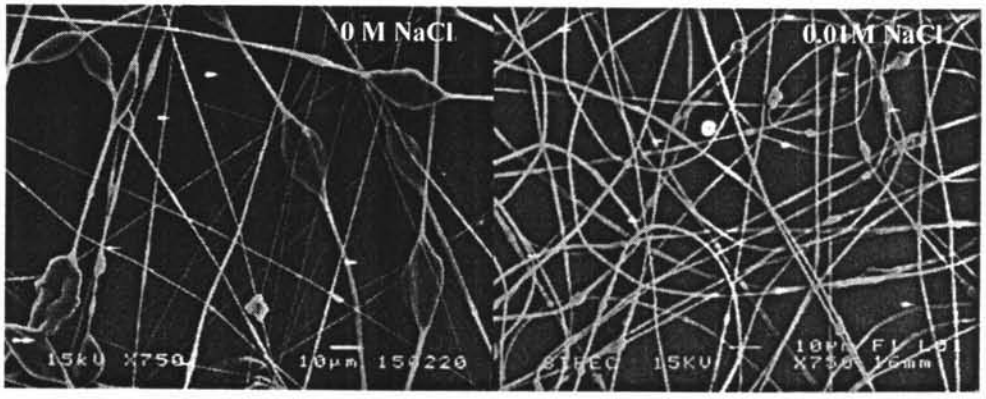

Figure 4.22 DSC profiles of as-synthesized PS-g-PCL 1:3 (a) and as-spun PS-g-PCL 1:3 (b).

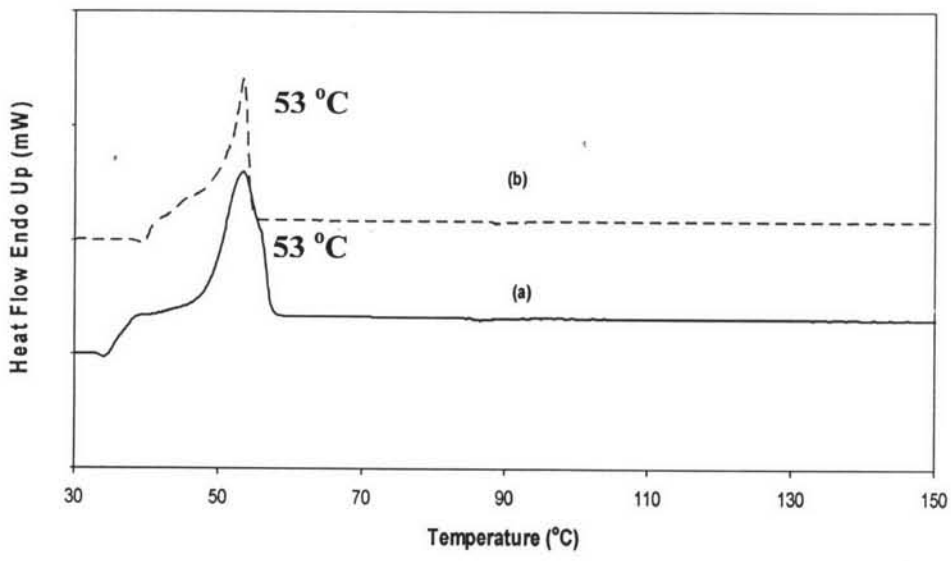

Figure 4.23 DSC profiles of as-synthesized PS-g-PCL 1:10 (a) and as-spun PS-g-PCL 1:10 (b).

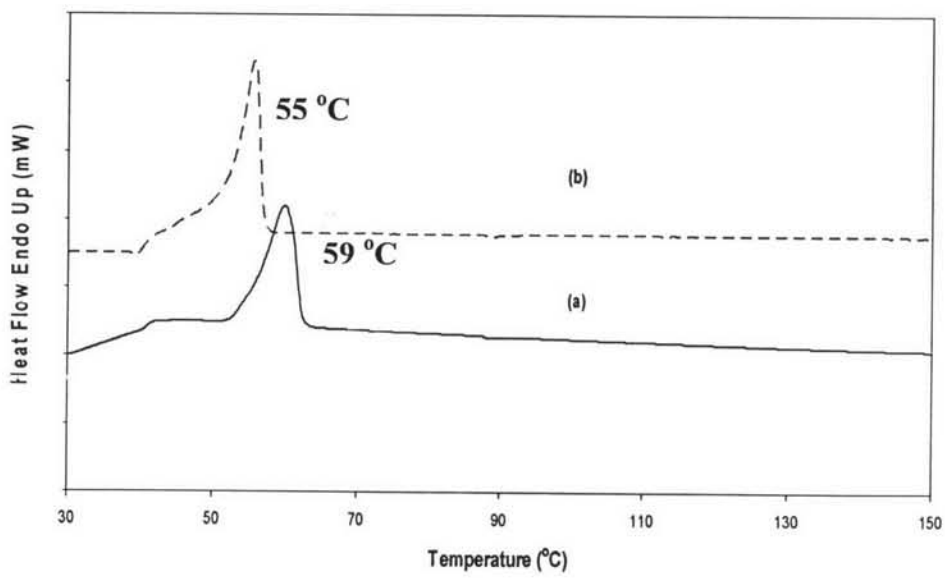

Figure 4.24 DSC profiles of as-synthesized PS-g-PCL 1:20 (a) and as-spun PS-g-PCL 1:20 (b).

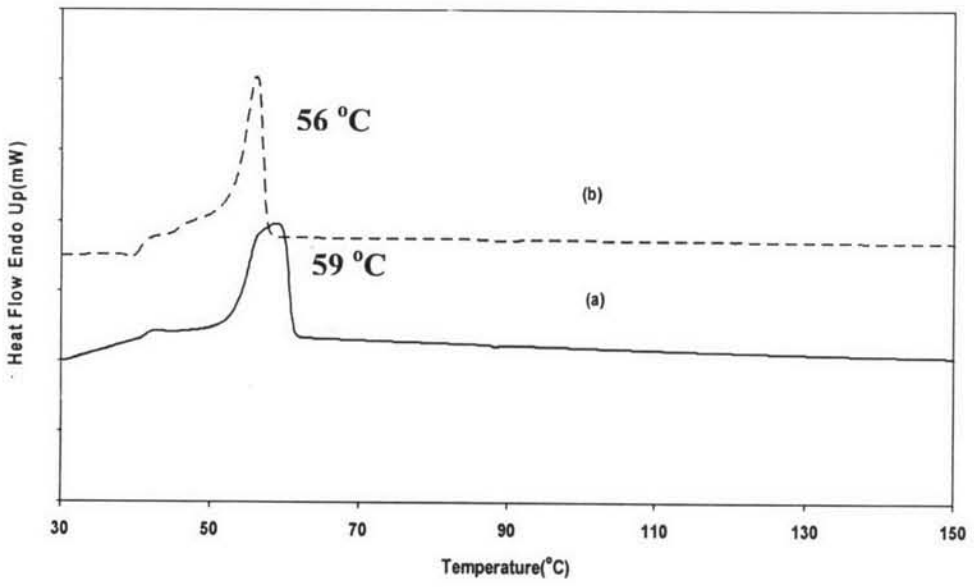

Figure 4.25 XRD patterns of as-synthesized PS-g-PCL 1:3 (a) and as-spun PS-g-PCL 1:3 (b).

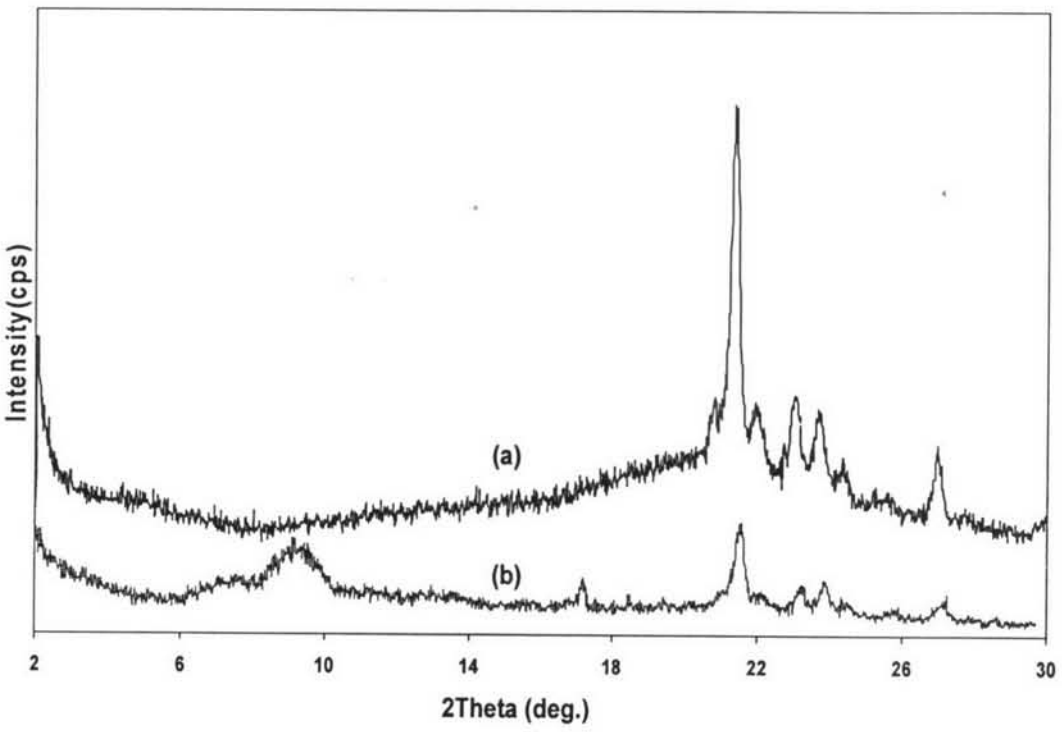

Figure 4.26 XRD patterns of as-synthesized PS-g-PCL 1:10 (a) and as-spun PS-g-PCL 1:10 (b).

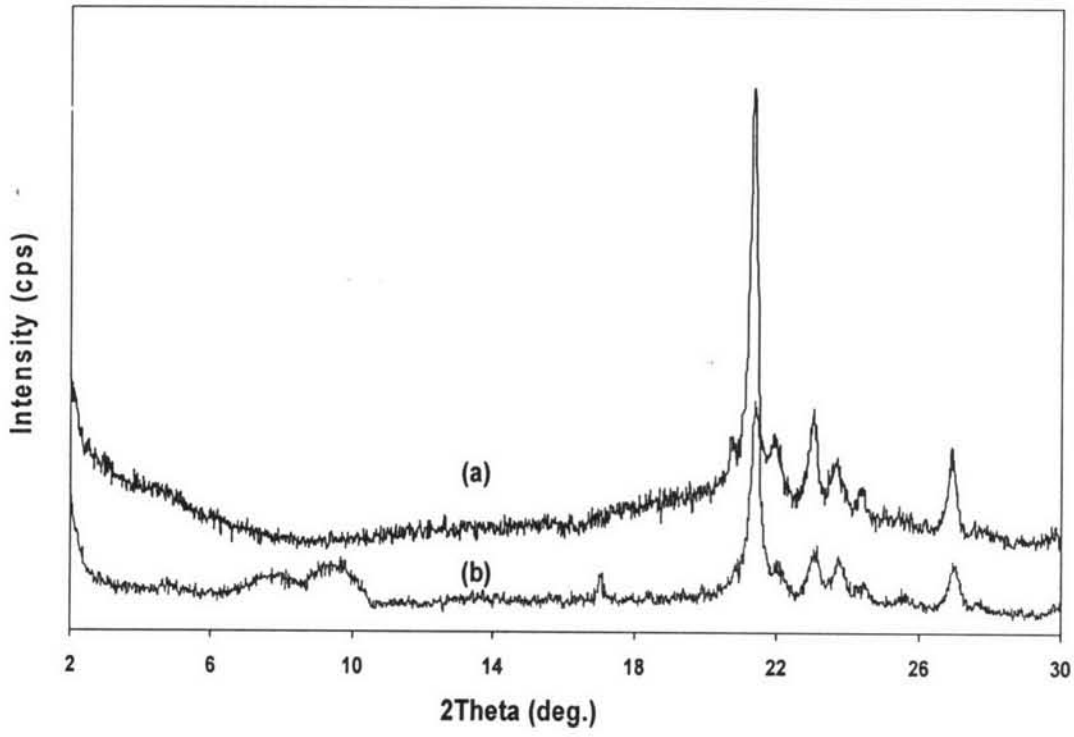

Figure 4.27 XRD patterns of as-synthesized PS-g-PCL 1:20 (a) and as-spun PS-g-PCL 1:20 (b).

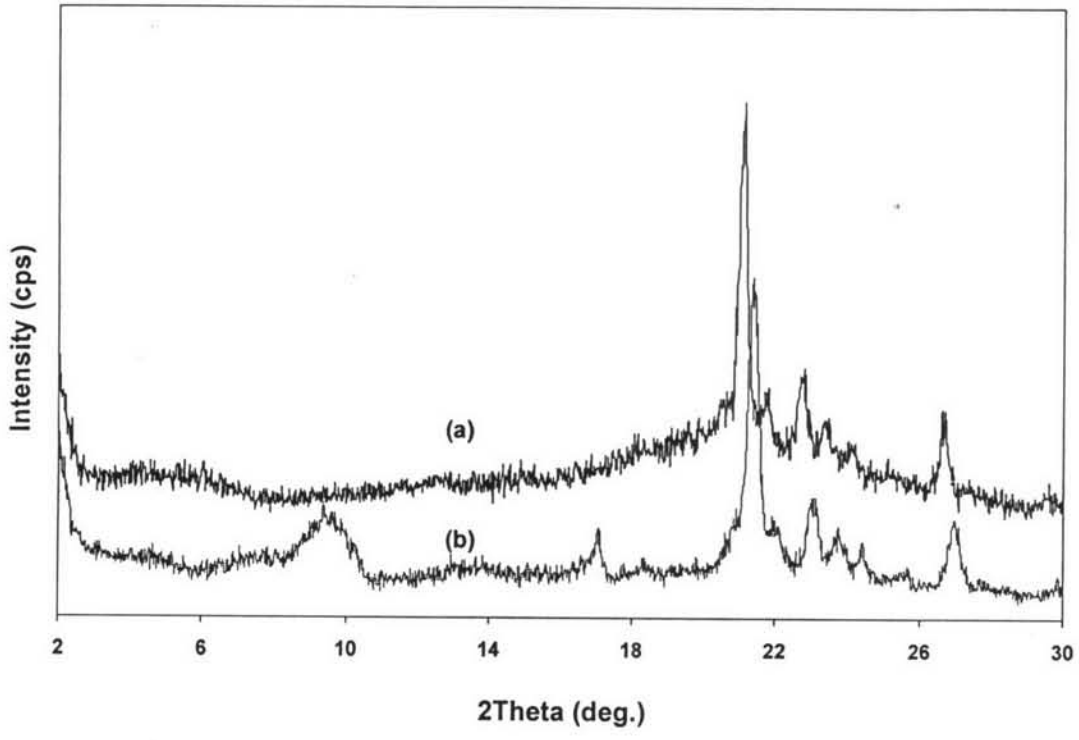

Figure 4.28 TG-DTA curve of PS-g-PCL at ratio 1:3.

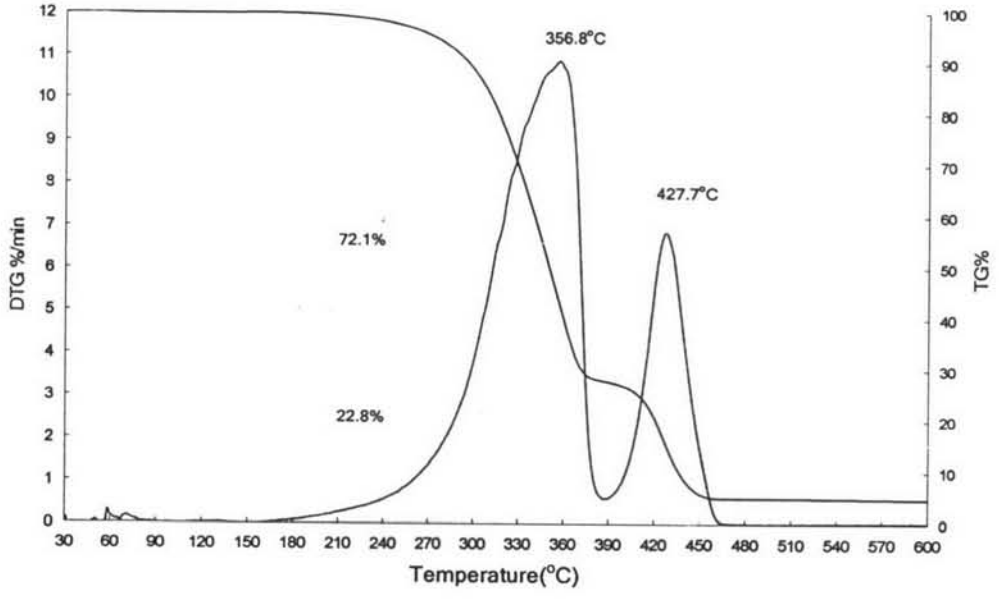

Figure 4.29 TG-DTA curve of PS-g-PCL at ratio 1:10.

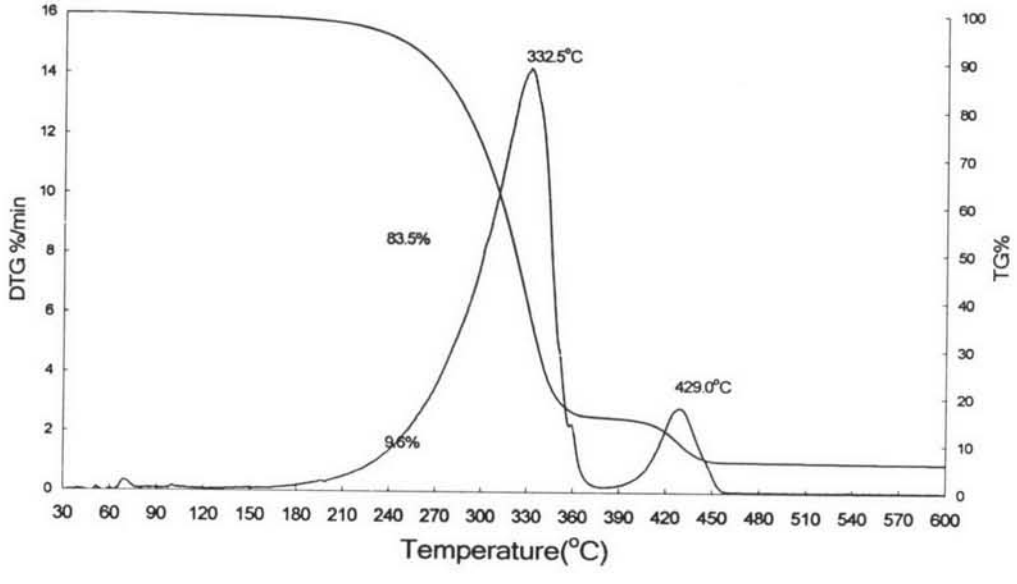

Figure 4.30 TG-DTA curve of PS-g-PCL at ratio 1:20.

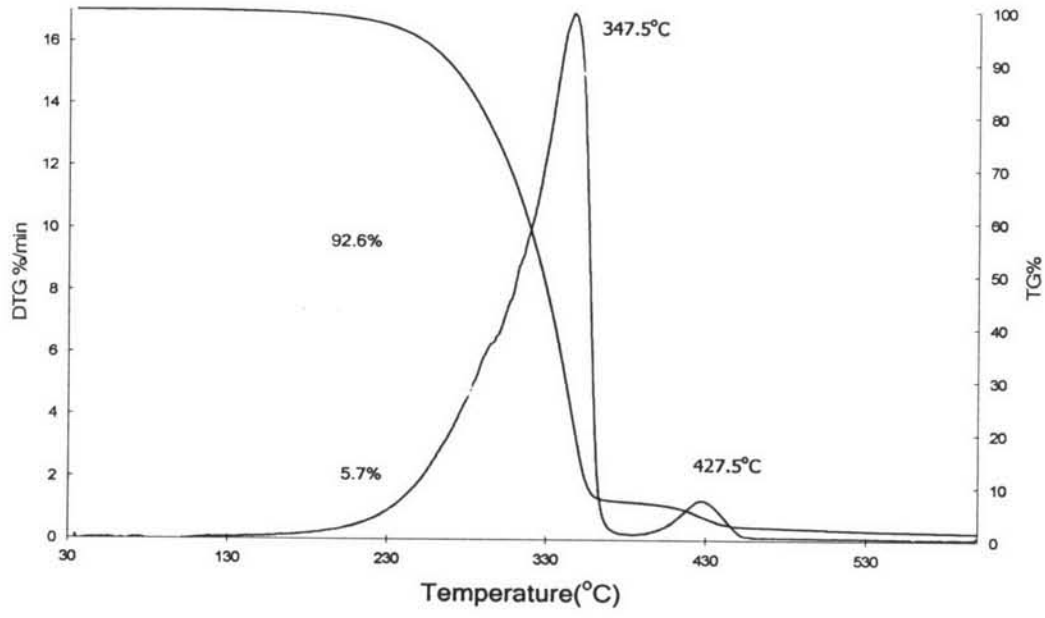

Figure 4.31 TG-DTA curve of electrospun PS-g-PCL at ratio 1:3, 30wt% at 15 kV.

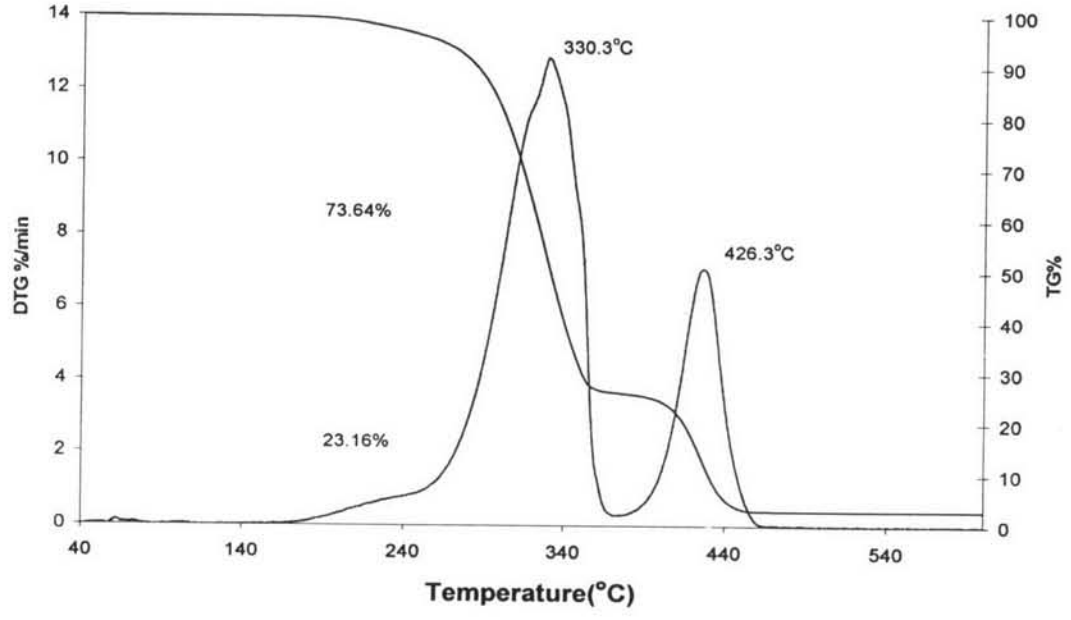

Figure 4.32 TG-DTA curve of electrospun PS-g-PCL at ratio 1:10, 30wt% at 15 kV.

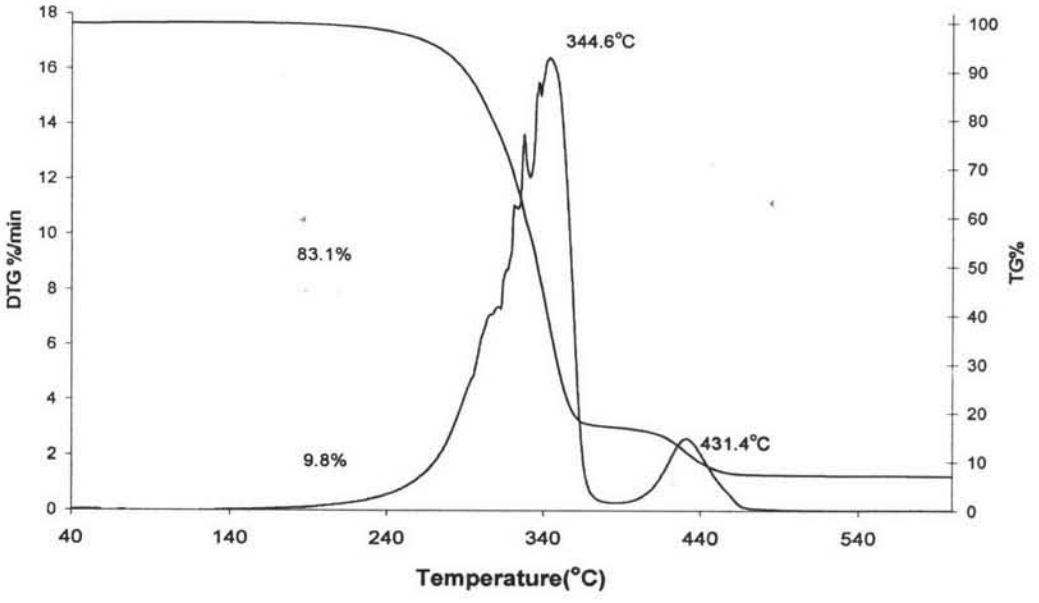

Figure 4.33 TG-DTA curve of electrospun PS-g-PCL at ratio 1:20, 30wt% at 15 kV.

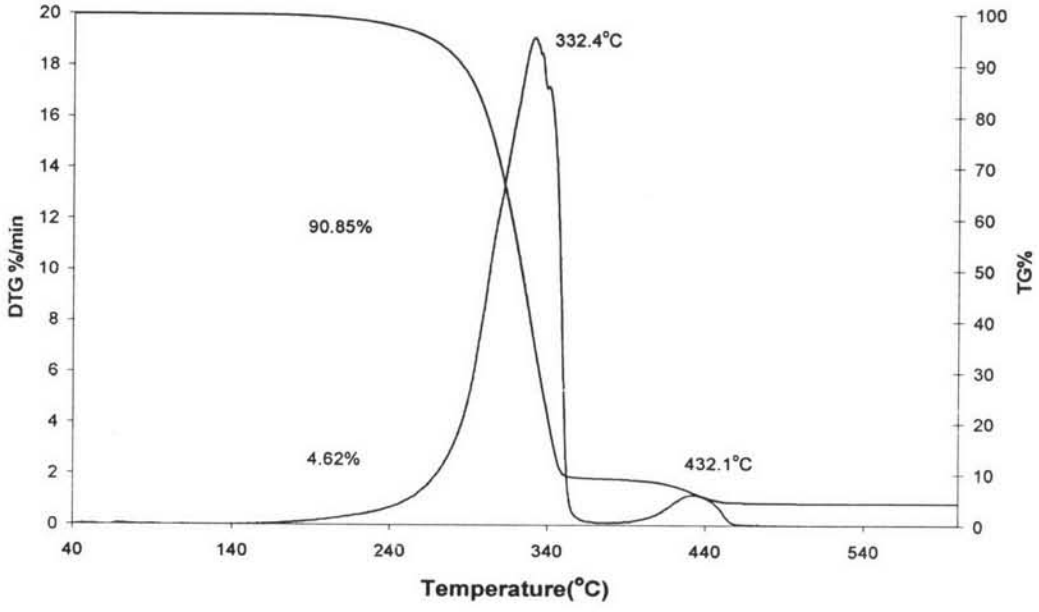

Figure 4.34 TG-DTA curve of PS-g-Nylon at ratio 1:1.

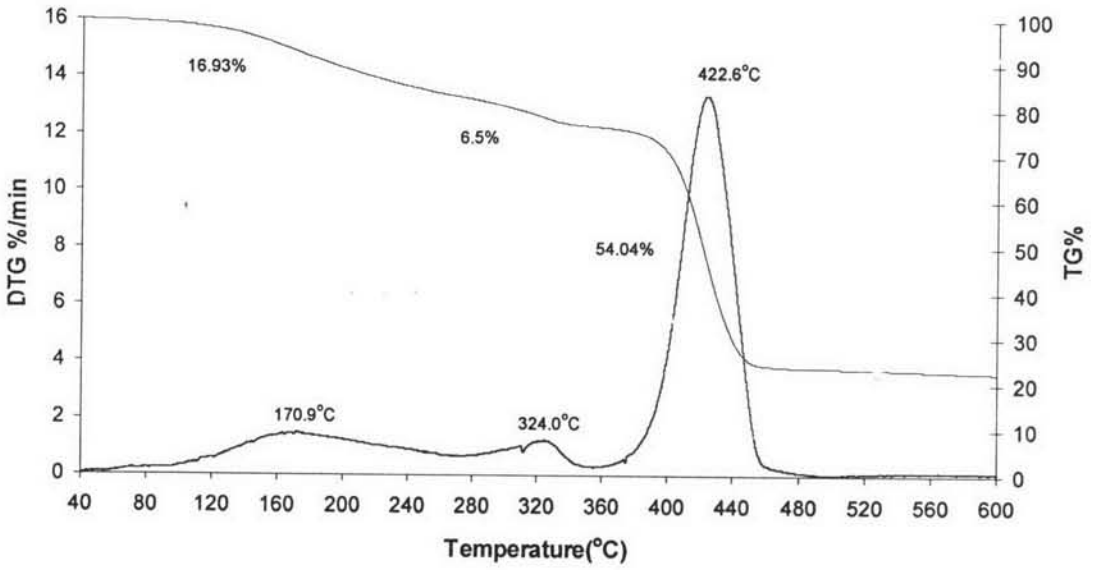

Figure 4.35 TG-DTA curve of PS-g-Nylon at ratio 1:2.

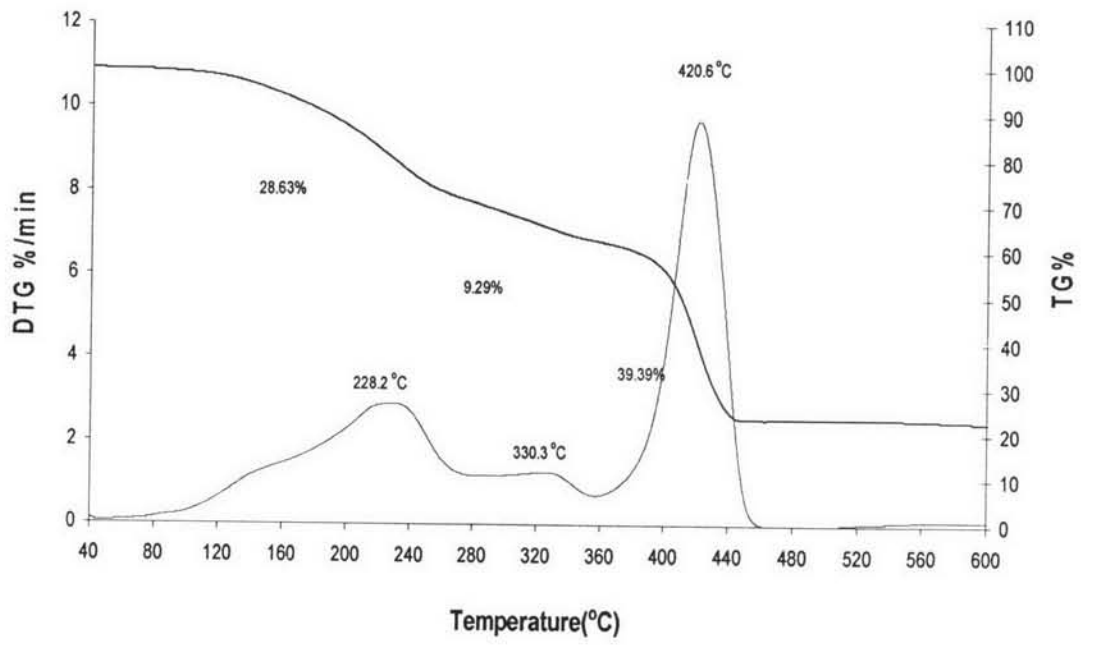

Figure 4.36 TG-DTA curve of PS-g-Nylon at ratio 1:3.

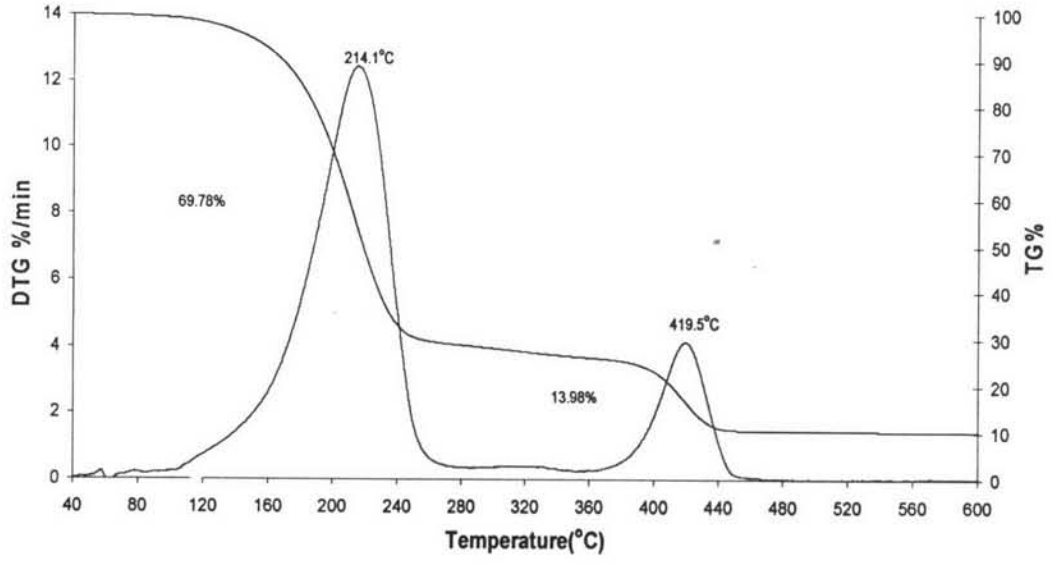

Figure 4.37 TG-DTA curve of electrospun PS-g-Nylon at ratio 1:1, 30wt% at 15 V.

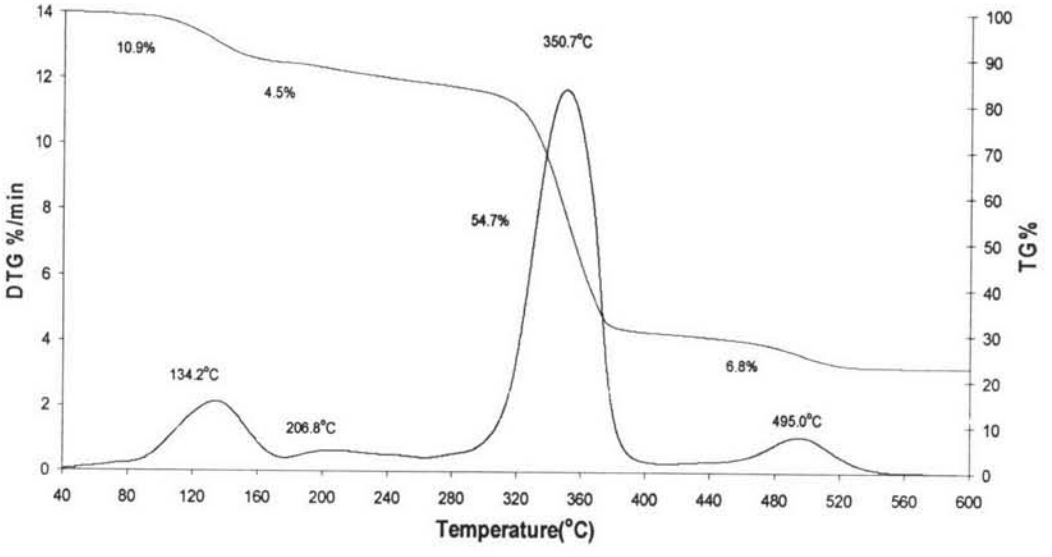

Figure 4.38 TG-DTA curve of electrospun PS-g-Nylon at ratio 1:2, 30wt% at 15 V.

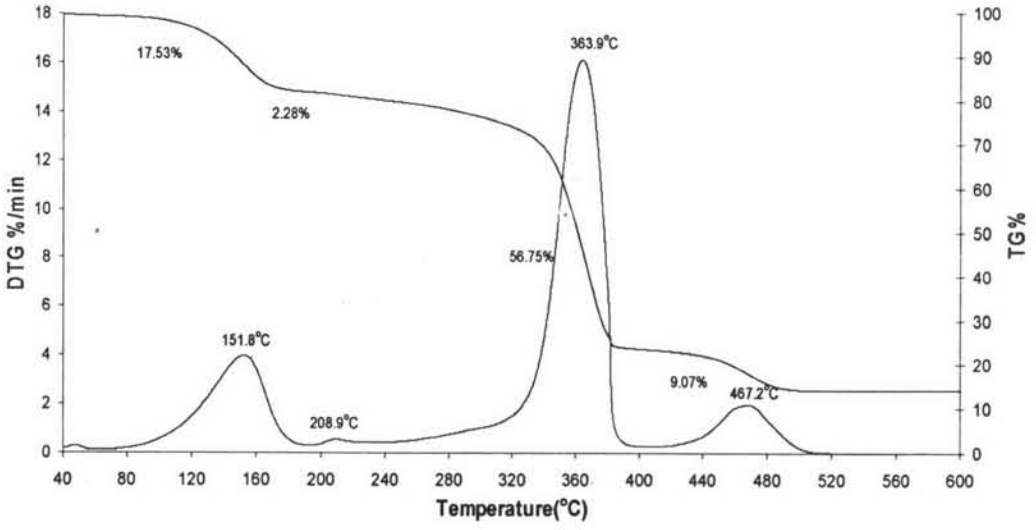

Figure 4.39 TG-DTA curve of electrospun PS-g-Nylon at ratio 1:3, 30wt% at 15 V.